Average Run Lengths of Control Charts for Autocorrelated Processes

by

Tung-Lung Wu

Advisor

Yung-Ming Chang

Institute of Statistics
National University of Kaohsiung
Kaohsiung, Taiwan 811

July, 2005

Table of Contents

List of Figures

List of Tables

具自我相關管制圖之平均連串長度

指導教授：張永明 博士

國立高雄大學應用數學系

學生：吳東隆

國立高雄大學統計學研究所

摘要

眾所週知，統計管制圖如修華特管制圖、累計和管制圖及指數加權移動平均管制圖已被廣泛的使用於改善產品和服務的品質，而平均連串長度爲一管制圖性能的傳統度量。通常求取連串長度之分佈及平均連串長度是一件困難且極爲繁瑣的工作。本篇論文之主旨在於以離散化和有限馬可夫嵌入法爲基礎，發展一簡單且有效能的方法用以探討具有自我相關管制圖的連串長度性質。此外，數值結果將用來說明我們的方法。

關鍵字：管制圖，平均連串長度，自我相關過程，馬可夫鏈嵌入，離散化。

Average Run Lengths of Control Charts for Autocorrelated Processes

Advisor: Dr. Yung-Ming Chang

Department of Applied Mathematics

National University of Kaohsiung

Student: Tung-Lung Wu

Institute of Statistics

National University of Kaohsiung

ABSTRACT

It is well known that statistical control charts such as Shewhart, CUSUM and EWMA charts have found widespread applications in improving the quality for manufacturing and service processes. The average run length is a traditional measurement of a control chart's performance. Usually, finding the run-length distribution and the average run length is a difficult and tedious task. In this thesis, we develop an unified approach based on the use of discretization and the finite Markov chain imbedding technique to investigate the run length properties of control charts when the observations have an autocorrelated structure. Numerical results are presented to illustrate our approach.

Keywords : Control chart, Average run length, Autoregressive process, Finite Markov chain imbedding, Discretization.

Chapter 1

Introduction

Control chart, one of the primary techniques of statistical process control (SPC), has been demonstrated to be an effective tool in reducing the variability and improving the quality of a process. It has been successfully used in many manufacturing and service processes. Shewhart chart, cumulative sum (CUSUM) chart and exponentially weighted moving average (EWMA) chart may be the most frequently studied control charts in the literature. Usually, assumptions concerning these charts are that the observations generated by the underlying process are independently and normally distributed with mean zero and variance σ^2. Unfortunately, such assumptions are sometimes violated in practice. In many manufacturing processes such as chemical processes, observations are always autocorrelated (see Montgomery, 2005). In the past decades, a considerable amount of contexts related to control charts in the presence of autocorrelation have been proposed. Some pertinent references include Johnson and Bagshaw (1974), Bagshaw and Johnson (1975), Bohm and Hackl (1996), Alwan and Robert (1988), Montgomery and Mastrangelo (1991), Harris and Ross (1991), Lu and Reynolds (1999, 2001), Yashchin (1993), Schmid (1997), VanBrackle and Reynolds (1997), Zhang (1998), Tseng and Adams (1994).

Traditionally, average run length (ARL) is the major criterion for measuring the performance of a control chart. When a chart is in control, it is always desirable to have a large ARL. On the other hand, a small ARL is preferable when an out of control condition has occurred in the chart. It has been found that the performance of traditional control charts is significantly affected by autocorrelated data. Two important effects of autocorrelation are that the in-control ARL becomes much smaller (except for Shewhart control charts) when the correlation is positive and the

out-of-control ARL becomes larger than expected. In words, it results in a higher false alarm rate and makes the shift in the process parameters more difficult to detect than that in the case of independent observations. Besides, when traditional control charts are applied to autocorrelated data, the traditional control limits are too tight and thus produce unnecessary false alarms. A large number of false alarms cause waste of costs and efforts for the unnecessary inspections in an in-control process.

Woodall and Faltin (1993) have suggested two strategies to deal with correlated processes. They indicated that the correlation should be eliminated if possible. However, since autocorrelation is often an inherent part of the processes and thus it must be properly modeled and monitored. There are two most widely used methods of treating autocorrelated processes. One is based on the residuals, while the other is based on the original observations. The idea of the residual-based scheme is to fit a time series model for the autocorrelated process. If the model is adequately fitted, the resulting residuals may be assumed to be normally distributed with mean zero and variance σ^2 in the absence of correlation. Therefore, the residuals can be monitored by the traditional control chart techniques without any modification. Wardell, Moskowitz and Plante (1994) compared the performance of Shewhart and EWMA control charts under an ARMA(1,1) model. Runger (1995) applied the residual-based technique to the CUSUM chart under the autoregressive (AR(p)) processes . Harris and Ross (1991), Lu and Reynolds (1999) and Montgomery and Mastrangelo (1991) analyzed several control charts applied to residuals.

The second method mentioned is to monitor the process by the original observations with adjusted control limits. Vasilopoulos and Stamboulis (1978) introduced a modified Shewhart chart for an AR(2) model. Zhang (1998) developed an EWMAST chart with modified control limits which depend on the correlated structure. Reynolds and Lu (1997) drew a conclusion that charts using residuals from a fitted time series model are not necessarily better than those based on the original observations with adjusted control limits unless the level of autocorrelation is quite high. It is more satisfactory to use a chart based on the original observations rather than

on the residuals. The scheme based on the original observations has the advantage that it is easier to understand and interpret for an operator.

VanBrackle and Reynolds (1997) used integral equation and Markov chain approaches to deal with the process modeled as AR(1) plus a random error. These two approaches are often used to calculate the ARL of a control chart. The Markov chain approach was first proposed by Brook and Evans (1972) to study the run length properties of a CUSUM chart under the assumption of independent and identically distributed (i.i.d.) observations. Yashchin (1993) pointed out that the presence of serial correlation destroys the Markov property of the monitoring statistic of the CUSUM scheme and the exact analysis becomes practically infeasible. This problem can be overcome by using the finite Markov chain imbedding (FMCI) approach introduced by Fu and Koutras (1994). In this thesis, our objective is to study the properties of control charts including Shewhart, CUSUM and EWMA charts based on the original observations by an unified FMCI approach for AR(1) and AR(2) models.

The rest of this thesis is organized as follows. In chapter 2, we introduce the idea of discretization and the method of FMCI. The autoregressive models AR(1) and AR(2) that are used to model the observations of the processes in the thesis are also briefly discussed. Under these two models, we investigate the run length properties of Shewhart control charts and Shewhart control charts with Western Electric rules in Chapter 3. Further, a comprehensive study on the run length for CUSUM and EWMA charts is given in Chapter 4. Finally, in Chapter 5, we compare the performances of Shewhart and EWMA charts that we study in Chapter 3 and Chapter 4. Numerical results are given and will be listed at the end of Chapter 3 to Chapter 5. In addition, simulation results based on generating 10,000 run lengths are also provided in the tables for each chart considered.

Chapter 2

Notations and Preliminaries

2.1 Finite Markov chain imbedding

Let $\{X_t\}$ be a sequence of observations of a random variable X (discrete or continuous) which represents certain quality characteristic and let random variable S_t be a monitoring statistic for a control chart. We define the run length variable for a control chart by

$$W = \inf\{t : S_t \text{ exceeds the control limits}\}. \tag{2.1}$$

Without loss of generality, we set the target value of process mean to be zero throughout the thesis. Further, we denote the in-control and out-of-control ARLs by ARL_0 and ARL_1, respectively.

We briefly describe the basic idea of the Markov chain approach proposed by Brook and Evans (1972) in the following. Suppose that a one-sided control chart is used. For a discrete monitoring statistic which takes $m+1$ values within the control limits, these values are treated as states of a Markov chain and all the values that exceed the limits are incorporated into an absorbing state. For a continuous monitoring statistic, the same idea is applied. The in-control area of a control chart is discretized into $m+1$ states and the state that exceeds the limits is treated as an absorbing state. As stated in Chapter 1, when observations are serial correlated, the Markov property for the monitoring statistics is destroyed. This problem can be tackled by introducing the FMCI technique. Fu, Spiring and Xie (2002) and Fu, Galit and Chang (2002) have developed an unified framework to find the ARLs for several control charts under the assumptions of normality and independence for observations. Their method includes two steps:

Step 1. Discretize the area of a one-sided (or two-sided) control chart into $m+2$ (or $2m+3$) states as Brook and Evans (1972) did. Then a sequence of discrete random variables (monitoring statistics) $S_t(m)$ can be obtained.

Step 2. Based on the monitoring statistics $S_t(m)$, one can construct a Markov chain $\{Y_t(m)\}$ that has a finite state space Ω and a transition matrix $\boldsymbol{M}(m)$ of the form

$$\boldsymbol{M}(m) = \left[\begin{array}{c|c} \boldsymbol{N}(m) & \boldsymbol{C}(m) \\ \hline \boldsymbol{0} & 1 \end{array}\right], \tag{2.2}$$

where $\boldsymbol{C}(m)$ is a column vector corresponding to the absorbing state.

Let $W(m)$ denote the run-length random variable induced by the finite Markov chain $\{Y_t(m)\}$. Then the probability, mean and standard deviation (SD) of run length can be obtained from the following results derived by Fu, Spiring and Xie (2002).

Theorem 2.1 *Given a positive integer m, we have*

(i) $P[W(m)=n] = \boldsymbol{\pi}_0(m)\boldsymbol{N}^{n-1}(m)(\boldsymbol{I}-\boldsymbol{N}(m))\boldsymbol{1}^\top$,

(ii) $E[W(m)] = \boldsymbol{\pi}_0(m)(\boldsymbol{I}-\boldsymbol{N}(m))^{-1}\boldsymbol{1}^\top$,

(iii) $E[W^2(m)] = \boldsymbol{\pi}_0(m)(\boldsymbol{I}+\boldsymbol{N}(m))(\boldsymbol{I}-\boldsymbol{N}(m))^{-2}\boldsymbol{1}^\top$,

where $\boldsymbol{\pi}_0(m) = (1,0,\ldots,0)$ is the initial distribution with 1 corresponding to a specified initial state, $\boldsymbol{I}$ is an identity matrix and $\boldsymbol{1}^\top$ is the transpose of the row vector $\boldsymbol{1} = (1,\ldots,1)$.

It has been shown that under mild conditions $S_t(m) \to S_t$ in distribution and $E[W^k(m)] \to E[W^k]$, $k = 1,2,\ldots$, as $m \to \infty$. Yashchin (1985) suggested that it would be satisfactory to use $m = 30$. This methodology can be easily extended to study the run-length properties for control charts in autocorrelated processes. The key is to incorporate the correlations into the construction of the Markov chain $\{Y_t(m)\}$ and settings of transition probabilities.

2.2 Process model assumptions

In this thesis, we assume that the underlying process has a AR(1) or AR(2) structure. These two models are briefly discussed in the successive sections.

2.2.1 First order autoregressive model

Suppose that the observations X_t, $t = 1, 2, \ldots$, are from an AR(1) process; that is, X_t satisfy the following relations:

$$X_t - \mu = \phi(X_{t-1} - \mu) + \varepsilon_t, \ t = 1, 2, \ldots, \tag{2.3}$$

where μ is the process mean, ϕ is the autoregressive parameter ($\mid \phi \mid < 1$) and ε_t is independent and normally distributed with mean zero and finite standard deviation σ_ε. Without loss of generality, we assume that $\mu = 0$ and $\sigma_\varepsilon = 1$. Furthermore, the starting value X_0 in model (2.3) is assumed to be either (i) normal with mean zero and variance $\frac{1}{1-\phi^2}$ or (ii) zero. For convenience, we denote model (2.3) by $\mathrm{AR^I}(1)$ under assumption (i) and by $\mathrm{AR^{II}}(1)$ under assumption (ii), respectively. From the assumption of X_0 in (i), we can deduce that the mean of X_t is given by

$$\begin{aligned} E(X_t) &= E(\phi X_{t-1} + \varepsilon_t) \ = \ \phi E(X_{t-1}) + 0 \ = \ \cdots \\ &= \phi^t E(X_0) \ = \ 0, \end{aligned}$$

and the variance of X_t is given by

$$\begin{aligned} V(X_t) &= V(\phi X_{t-1} + \varepsilon_t) \ = \ \phi^2 V(X_{t-1}) + 1 \ = \ \cdots \\ &= V(\phi^t X_0) + \phi^{2t-2} + \cdots + 1 \\ &= \phi^{2t} \cdot \frac{1}{1-\phi^2} + \frac{1-\phi^{2t}}{1-\phi^2} \\ &= \frac{1}{1-\phi^2}. \end{aligned} \tag{2.4}$$

for $t = 1, 2, \ldots$. This results in a stationary AR(1) process; that is, $X_t \sim N\left(0, \frac{1}{1-\phi^2}\right)$ for all t.

2.2.2 Second order autoregressive model

Suppose that the observations X_t, $t = 2, 3, \ldots$, are from an AR(2) process; that is, X_t satisfy the following relations:

$$X_t - \mu = \phi_1(X_{t-1} - \mu) + \phi_2(X_{t-2} - \mu) + \varepsilon_t, \ t = 2, 3, \ldots, \tag{2.5}$$

where μ is the process mean, ϕ_1 and ϕ_2 are the autoregressive parameters that have the following restrictions

$$\phi_1 + \phi_2 < 1, \quad \phi_1 - \phi_2 < 1, \quad -1 < \phi_2 < 1, \tag{2.6}$$

and $\varepsilon_t \sim$ i.i.d. $N(0, 1)$. In model (2.5), we consider two assumptions for the starting values X_0 and X_1:

(i) X_0 and X_1 are from a bivariate normal distribution with marginal mean 0, marginal variance $\frac{1-\phi_2}{(1+\phi_2)(1-\phi_2+\phi_1)(1-\phi_2-\phi_1)}$ and covariance $E(X_0X_1) = \frac{\phi_1}{(1-\phi_2)}$.

(ii) X_0 is assumed to be zero and X_0 and X_1 have a relation given by (2.4); that is, $X_1 = \phi X_0 + \varepsilon_1 = \varepsilon_1$.

Again, we use the notations $\mathrm{AR}^{\mathrm{I}}(2)$ and $\mathrm{AR}^{\mathrm{II}}(2)$ to denote the model given by (2.5) under assumptions (i) and (ii), respectively. It can be shown that assumption (i) leads to a stationary AR(2) process; more specifically, $X_t \sim N\left(0, \frac{1-\phi_2}{(1+\phi_2)(1-\phi_2+\phi_1)(1-\phi_2-\phi_1)}\right)$ and the covariance of X_{t-1} and X_t is $E(X_{t-1}X_t) = \frac{\phi_1}{(1-\phi_2)}$ for all t .

Chapter 3

Shewhart Control Charts for Autocorrelated Processes

In this chapter, we follow the two steps described in Section 2.1 to study the run-length properties of Shewhart control charts and Shewhart control charts with Western Electric rules when observations are from AR(1) and AR(2) processes. All the findings are new.

3.1 Average run lengths for AR(1) process

It is known that the monitoring statistic for a Shewhart control chart is the observation X_t itself and the condition for signaling an alarm is that the present observation exceeds some control limits; i.e. $|X_t| \geq h$ for some $h > 0$. Assume that X_t, $t = 1, 2, \ldots$, are from a $\mathrm{AR}^{\mathrm{I}}(1)$ process, that is,

$$X_t = \phi X_{t-1} + \varepsilon_t, \tag{3.1}$$

where ϕ is the autoregressive parameter, $\varepsilon_t \sim$ i.i.d. $N(0,1)$ and $X_t \sim N\left(0, \frac{1}{1-\phi^2}\right)$ for all t. To find the run-length distributions, we provide details for the discretization and imbedding procedures in the following.

Step 1: Discretization

Given a positive integer m, each side of the control chart is discretized into m states plus one state that exceeds the control limit (h or $-h$). States are assumed to be equally spaced with a small distance $\Delta > 0$ (usually $\Delta = \frac{h}{(m+1)-0.5}$). Let $D(X)$ be the discretized random variable X in the following sense,

$$D(X) = i\Delta, \ i = 0, \pm 1, \ldots, \pm m, \pm(m+1), \tag{3.2}$$

We define the probabilities $p_i \equiv P(D(X) = i\Delta)$ as follows :

$$\begin{aligned} p_i &= \int_{(i-0.5)\Delta}^{(i+0.5)\Delta} f(x)\,dx,\ \ i = 0, \pm 1, \ldots, \pm m, \\ p_{m+1} &= \int_{[(m+1)-0.5]\Delta}^{\infty} f(x)\,dx,\ \ and \\ p_{-(m+1)} &= \int_{-\infty}^{[-(m+1)+0.5]\Delta} f(x)\,dx. \end{aligned} \tag{3.3}$$

where $f(x)$ is the density function of X.

Step 2: Imbedding

For simplicity, we denote $D(X_t) = i\Delta$ as $D(X_t) = i$. In the $\mathrm{AR}^{\mathrm{I}}(1)$ process, we have assumed that the starting value X_0 is from $N\left(0, \frac{1}{1-\phi^2}\right)$. Thus, an out of control signal could occurr at the stage of X_0 and hence this stage should be taken into account when computing the ARL. For this purpose, it is reasonable to introduce a dummy variable X_{-1} and define an initial state $D(X_{-1}) = \emptyset$ with $P(D(X_{-1}) = \emptyset) = 1$. Now define a state space Ω by

$$\Omega = \{\emptyset, -m, \ldots, -1, 0, 1, \ldots, m, \alpha\}. \tag{3.4}$$

Note that the states $\pm(m+1)$ are combined into an absorbing state α. Obviously, $\mathrm{card}(\Omega) = 2m + 3$. For $t \geq -1$, we define a Markov chain $\{Y_t(m)\}$ that takes values on the state space Ω by

$$Y_t(m) = D(X_t). \tag{3.5}$$

It follows from (3.4) and (3.5) that the transition probabilities $p_{ij},\ i, j \in \Omega$, for the imbedded Markov chain $\{Y_t(m)\}$ can be specified as follows: for $t = 0$, we have

(1) if $i = \emptyset$ and $j = 0, \pm 1, \ldots, \pm m$, then

$$\begin{aligned} p_{ij} &= P(Y_0(m) = j \mid Y_{-1}(m) = i) \\ &= P((j - 0.5)\Delta \leq X_0 \leq (j + 0.5)\Delta), \end{aligned}$$

(2) if $i = \emptyset$ and $j = \alpha$, then

$$\begin{aligned} p_{ij} &= P(Y_0(m) = j \mid Y_{-1}(m) = i) \\ &= P(X_0 \geq ((m+1) - 0.5)\Delta \text{ or } X_0 \leq (-(m+1) + 0.5)\Delta) \\ &= P(X_0 \geq (m + 0.5)\Delta) + P(X_0 \leq (-m - 0.5)\Delta), \end{aligned}$$

where $X_0 \sim N\left(0, \frac{1}{1-\phi^2}\right)$, and for $t \geq 1$, we have

(3) if $i, j = 0, \pm 1, \ldots, \pm m$, then

$$\begin{aligned} p_{ij} &= P(Y_t(m) = j \mid Y_{t-1}(m) = i) \\ &= P((j-0.5)\Delta \leq X_t \leq (j+0.5)\Delta \mid X_{t-1} = i\Delta) \\ &= P((j-0.5)\Delta \leq \phi X_{t-1} + \varepsilon_t \leq (j+0.5)\Delta \mid X_{t-1} = i\Delta) \\ &= P((j-\phi i-0.5)\Delta) \leq \varepsilon_t \leq (j-\phi i+0.5)\Delta) \\ &= \Phi((j-\phi i+0.5)\Delta) - \Phi((j-\phi i-0.5)\Delta), \end{aligned}$$

(4) if $i = 0, \pm 1, \ldots, \pm m$ and $j = \alpha$, then

$$\begin{aligned} p_{ij} &= P(Y_t(m) = \alpha \mid Y_{t-1}(m) = i) \\ &= P(X_t \geq ((m+1)-0.5)\Delta \text{ or } X_t \leq (-(m+1)+0.5)\Delta \mid X_{t-1} = i\Delta) \\ &= P(\varepsilon_t \geq (m+0.5-\phi i)\Delta \text{ or } \varepsilon_t \leq (-m-0.5-\phi i)\Delta) \\ &= \Phi((-m-0.5-\phi i)\Delta) + 1 - \Phi((m+0.5-\phi i)\Delta), \end{aligned}$$

(5) if $i = \alpha$ and $j = 0, \pm 1, \ldots, \pm m$, then

$$p_{ij} = 0,$$

(6) if $i, j = \alpha$, then

$$p_{ij} = 1,$$

where $\Phi(x)$ denotes the cumulative density function of the standard normal distribution. Thus, the transition probability matrix $\boldsymbol{M}(m) = (p_{ij})$ can be obtained and written in the form given by (2.2) and the exact probability, mean and standard deviation of run length can be evaluated by Theorem 2.1.

Next, suppose an $\mathrm{AR}^{\text{II}}(1)$ process is under consideration. In this case, the procedures for the two steps above are almost the same. The only difference is that we assume that the starting value X_0 is at the initial state $\emptyset$ with probability one; i.e. $P(X_0 = \emptyset) = 1$ and hence the transition probabilities p_{ij} for $i = \emptyset$ and

$j = 0, \pm 1, \ldots, \pm m, \alpha$, are generated from the standard normal distribution $N(0,1)$. Generally speaking, the ARL for a Shewhart control chart in an $\mathrm{AR}^{\mathrm{I}}(1)$ process is a little bit smaller than that in an $\mathrm{AR}^{\mathrm{II}}(1)$ process. We provide a simple example to make the method more transparent.

Example 3.1 Consider a Shewhart control chart with observations from the $\mathrm{AR}^{\mathrm{II}}(1)$ process. Take $h = 3$ and $m = 2$ then $\Delta = \frac{3}{2.5}$. Following the discretization and imbedding procedures, we can define a Markov chain $\{Y_t(2)\}$ taking values on the state space $\Omega = \{0, \pm 1, \pm 2, \alpha\}$ (± 3 are combined into the absorbing state α). The submatrix $\boldsymbol{N}(2)$ of the transition matrix $\boldsymbol{M}(2)$ is given by

$$\boldsymbol{N}(2) = \begin{array}{c} \\ \emptyset \\ -2 \\ -1 \\ 0 \\ 1 \\ 2 \end{array} \begin{bmatrix} 0 & p_{-2} & p_{-1} & p_0 & p_1 & p_2 \\ 0 & p_{-2,-2} & p_{-2,-1} & p_{-2,0} & p_{-2,1} & p_{-2,2} \\ 0 & p_{-1,-2} & p_{-1,-1} & p_{-1,0} & p_{-1,1} & p_{-1,2} \\ 0 & p_{0,-2} & p_{0,-1} & p_{0,0} & p_{0,1} & p_{0,2} \\ 0 & p_{1,-2} & p_{1,-1} & p_{1,0} & p_{1,1} & p_{1,2} \\ 0 & p_{2,-2} & p_{2,-1} & p_{2,0} & p_{2,1} & p_{2,2} \end{bmatrix}.$$

where $p_i,\ i = 0, \pm 1, \pm 2$, are generated from $N(0,1)$ and p_{ij}'s are computed by the equations derived in (3)-(6). With $\phi = 0.5$, Table 3.1 shows the mean and standard deviation of the run length at different levels of discretization (m). It is clear that the numerical results are rather stable for $m \geq 30$.

In the above example, we took ± 3 to be the control limits. It can be seen from Table 3.1 that these limits are too tight and thus result in a smaller in-control ARL. In fact, they are only suitable for i.i.d. observations. When autocorrelation is presented in the observations, the control limits should be adjusted to be $\pm 3\sigma_x$ where $\sigma_x^2 = \frac{1}{1-\phi^2}$. In Table 3.2, we compare the ARLs using the control limit $h = 3$ with the ARLs using the control limit $h = 3\sigma_x$. Clearly, the ARL_0's with $h = 3$ drop dramatically when the autoregressive parameter ϕ is getting larger. In this situation, we will observe a large amount of false alarms in the control chart. On the other hand, the use of the adjusted limit $h = 3\sigma_x$ does increase the values of ARL_0's. This prevents from waste of costs for unnecessary inspections in the

process. In the rest of this chapter and the successive chapters, we shall use the adjusted limit $h = 3\sigma_x$ in each chart considered.

Tables 3.3 and 3.4 give the ARLs for $\mathrm{AR}^{\mathrm{I}}(1)$ and $\mathrm{AR}^{\mathrm{II}}(1)$ processes with various magnitudes of ϕ and shifts ξ. We see that the ARL_1's become larger when the correlation gets higher. This reduces the performance of the control chart.

3.2 Average run lengths for AR(2) process

Assume first that the observations X_t, $t = 2, 3, \ldots$, are from a $\mathrm{AR}^{\mathrm{I}}(2)$ process; that is,

$$X_t = \phi_1 X_{t-1} + \phi_2 X_{t-2} + \varepsilon_t, \tag{3.6}$$

where ϕ_1 and ϕ_2 are the autoregressive parameters and $\varepsilon_t \sim$ i.i.d. $N(0,1)$ and $X_t \sim N\left(0, \frac{(1-\phi_2)}{(1+\phi_2)(1-\phi_2+\phi_1)(1-\phi_2-\phi_1)}\right)$ for each t. We apply the methodology used in the previous section to find the run-length distributions of a Shewhart control chart for model (3.6).

Step 1: Discretization

The discretization procedure is the same as the procedure described in Section 3.1 except that the probabilities $p_i \equiv P(D(X) = i\Delta),\ i = 0, \pm 1, \ldots, \pm m, \pm(m+1)$, are determined by the normal distribution $N\left(0, \frac{(1-\phi_2)}{(1+\phi_2)(1-\phi_2+\phi_1)(1-\phi_2-\phi_1)}\right)$.

Step 2: Imbedding

In model (3.6), we have assumed that the starting values X_0 and X_1 are from a bivariate normal distribution and thus these two stages should be taken into account when computing the run-length distributions for the same reason stated in Section 3.1. Therefore, two dummy variables X_{-1} and X_{-2} are needed so that the desired Markov chain can be constructed properly. Define an initial state $(D(X_{-2}), D(X_{-1})) = (\emptyset, \emptyset)$ with $P((D(X_{-2}), D(X_{-1})) = (\emptyset, \emptyset)) = 1$. According to the structure of the $\mathrm{AR}^{\mathrm{I}}(2)$ process, we define a state space Ω as

$$\begin{aligned}\Omega \;=\; & \{(\emptyset,\emptyset), (\emptyset,-m), \ldots, (\emptyset,m), (-m,-m), \ldots, (-m,m), (-m+1,-m), \\ & \ldots, (-m+1,m), \ldots, (m,-m), \ldots (m,m), \alpha\},\end{aligned} \tag{3.7}$$

with $(2m+1)(2m+2)+2$ states in total. Note that states that include $\pm(m+1)$ as one of coordinates are combined into an absorbing state α. We define a Markov chain $\{Y_t(m)\}$ that takes values on the state space Ω by

$$Y_t(m) = [D(X_{t-1}), D(X_t)]. \tag{3.8}$$

It follows from (3.7) and (3.8) that the transition probabilities from state (i_{t-2}, i_{t-1}) at time $t-1$ to state (i_{t-1}, i_t) at time t for the imbedded Markov chain $\{Y_t(m)\}$ can be specified as follows:

(1) if $u = (\emptyset, \emptyset)$, $v = (\emptyset, i_0)$ and $i_0 = 0, \pm 1, \ldots, \pm m$, then

$$\begin{aligned} p_{uv} &= P(Y_0(m) = v \mid Y_{-1}(m) = u) \\ &= P((i_t - 0.5)\Delta \le X_0 \le (i_t + 0.5)\Delta), \end{aligned}$$

where $X_0 \sim N\left(0, \frac{(1-\phi_2)}{(1+\phi_2)(1-\phi_2+\phi_1)(1-\phi_2-\phi_1)}\right)$,

(2) if $u = (\emptyset, \emptyset)$ and $v = \alpha$, then

$$\begin{aligned} p_{uv} &= P(Y_0(m) = v \mid Y_{-1}(m) = u) \\ &= P(X_0 \ge (m + 1 - 0.5)\Delta \text{ or } X_0 \le (-m - 1 + 0.5)\Delta) \\ &= P(X_0 \ge (m + 0.5)\Delta) + P(X_0 \le (-m - 0.5)\Delta), \end{aligned}$$

(3) if $u = (\emptyset, i_0)$, $v = (i_0, i_1)$ and $i_0, i_1 = 0, \pm 1, \ldots, \pm m$, then

$$\begin{aligned} p_{uv} &= P(Y_1(m) = v \mid Y_0(m) = u) \\ &= P(X_1 = i_1\Delta \mid X_0 = i_0\Delta), \end{aligned}$$

where $X_1 \mid X_0 = i_0\Delta \sim N(\phi(i_0\Delta), (1-\phi^2)\sigma_x^2)$,

(4) if $u = (\emptyset, i_0)$, $v = \alpha$ and $i_0 = 0, \pm 1, \ldots, \pm m$, then

$$\begin{aligned} p_{uv} &= P(Y_1(m) = v \mid Y_0(m) = u) \\ &= P(X_1 \ge (m + 0.5)\Delta \text{ or } X_1 \le (-m - 0.5)\Delta \mid X_0 = i_0\Delta) \\ &= P(X_1 \ge (m + 0.5)\Delta \mid X_0 = i_0\Delta) + P(X_1 \le (-m - 0.5)\Delta \mid X_0 = i_0\Delta), \end{aligned}$$

(5) if $u = (i_{t-2}, i_{t-1})$, $v = (i_{t-1}, i_t)$ and $i_{t-2}, i_{t-1}, i_t = 0, \pm 1, \ldots, \pm m$, for $t \geq 2$, then

$$\begin{aligned}
p_{uv} &= P(Y_t(m) = v \mid Y_{t-1}(m) = u) \\
&= P((i_t - 0.5)\Delta \leq X_t \leq (i_t + 0.5)\Delta \mid X_{t-1} = i_{t-1}\Delta,\ X_{t-2} = i_{t-2}\Delta) \\
&= P((i_t - 0.5)\Delta \leq \phi_1 X_{t-1} + \phi_2 X_{t-2} + \varepsilon_t \leq (i_t + 0.5)\Delta \mid \\
&\quad X_{t-1} = i_{t-1}\Delta, X_{t-2} = i_{t-2}\Delta) \\
&= P((i_t - 0.5 - \phi_1 i_{t-1} - \phi_2 i_{t-2})\Delta \leq \varepsilon_t \leq (i_t + 0.5 - \phi_1 i_{t-1} - \phi_2 i_{t-2})\Delta) \\
&= \Phi((i_t + 0.5 - \phi_1 i_{t-1} - \phi_2 i_{t-2})\Delta) - \Phi((i_t - 0.5 - \phi_1 i_{t-1} - \phi_2 i_{t-2})\Delta),
\end{aligned}$$

where Φ is the cumulative density function of the standard normal distribution,

(6) if $u = (i_{t-2}, i_{t-1})$, $v = \alpha$ and $i_{t-2}, i_{t-1} = 0, \pm 1, \ldots, \pm m$, for $t \geq 2$, then

$$\begin{aligned}
p_{uv} &= P(Y_t(m) = v \mid Y_{t-1}(m) = u) \\
&= P(X_t \geq (m + 1 - 0.5)\Delta \text{ or } X_t \leq (-(m+1) + 0.5)\Delta \mid \\
&\quad X_{t-1} = i_{t-1}\Delta,\ X_{t-2} = i_{t-2}\Delta) \\
&= P(\phi_1 X_{t-1} + \phi_2 X_{t-2} + \varepsilon_t \geq (m + 0.5)\Delta \text{ or } \phi_1 X_{t-1} + \phi_2 X_{t-2} + \\
&\quad \varepsilon_t \leq (-m - 0.5)\Delta \mid X_{t-1} = i_{t-1}\Delta,\ X_{t-2} = i_{t-2}\Delta) \\
&= P(\varepsilon_t \geq (m + 0.5 - \phi_1 i_{t-1} - \phi_2 i_{t-2})\Delta \text{ or} \\
&\quad \varepsilon_t \leq (-m - 0.5 - \phi_1 i_{t-1} - \phi_2 i_{t-2})\Delta) \\
&= \Phi((-m - 0.5 - \phi_1 i_{t-1} - \phi_2 i_{t-2})\Delta) + 1 \\
&\quad -\Phi((m + 0.5 - \phi_1 i_{t-1} - \phi_2 i_{t-2})\Delta),
\end{aligned}$$

(7) if $v = (i_{t-1}, i_t)$ and $i_{t-1}, i_t = 0, \pm 1, \ldots, \pm m$, for $t \geq 1$, then $p_{\alpha v} = 0$,

(8) $p_{\alpha\alpha} = 1$.

Next, suppose the observations X_t, $t = 2, 3, \ldots$, are from an $\mathrm{AR}^{\mathrm{II}}(2)$ process. Recall that the assumptions for this process are that $X_0 = 0$ and X_0 and X_1 follow an AR(1) model; i.e. $X_1 = \varepsilon_1 \sim N(0, 1)$. According to these assumptions, we only need a dummy variable X_{-1} to construct the state space for the imbedded Markov chain $Y_t(m)$. Define $D(X_{-1}) = \emptyset$ with probability one. Then the state space Ω of

the imbedded Markov chain $Y_t(m)$ for $\mathrm{AR}^{\mathrm{II}}(2)$ process is defined by

$$\begin{aligned}\Omega &= \{(\emptyset,0),(-m,-m),\ldots,(-m,m),(-m+1,-m),\ldots,(-m+1,m),\\ &\quad \ldots,(m,-m),\ldots(m,m),\alpha\}. \end{aligned} \tag{3.9}$$

Example 3.2 Consider a Shewhart control chart in the $\mathrm{AR}^{\mathrm{II}}(2)$ process. We choose the control limit $h = 3\sigma_x$ and $m = 1$. Then the submatrix $\boldsymbol{N}(1)$ of the transition matrix $\boldsymbol{M}(1)$ is given by

$$\begin{array}{c} \begin{array}{cccccccccc} (\emptyset,0) & (-1,-1) & (-1,0) & (-1,1) & (0,-1) & (0,0) & (0,1) & (1,-1) & (1,0) & (1,1) \end{array} \\ \left[\begin{array}{cccccccccc} 0 & 0 & 0 & 0 & p_{-1} & p_0 & p_1 & 0 & 0 & 0 \\ 0 & p_{-1,-1,-1} & p_{-1,-1,0} & p_{-1,-1,1} & 0 & 0 & 0 & 0 & 0 & \\ 0 & 0 & 0 & 0 & p_{-1,0,-1} & p_{-1,0,0} & p_{-1,0,1} & 0 & 0 & 0 \\ 0 & 0 & 0 & 0 & 0 & 0 & 0 & p_{-1,1,-1} & p_{-1,1,0} & p_{-1,1,1} \\ 0 & p_{0,-1,-1} & p_{0,-1,0} & p_{0,-1,1} & 0 & 0 & 0 & 0 & 0 & \\ 0 & 0 & 0 & 0 & p_{0,0,-1} & p_{0,0,0} & p_{0,0,1} & 0 & 0 & 0 \\ 0 & 0 & 0 & 0 & 0 & 0 & 0 & p_{0,1,-1} & p_{0,1,0} & p_{0,1,1} \\ 0 & p_{1,-1,-1} & p_{1,-1,0} & p_{1,-1,1} & 0 & 0 & 0 & 0 & 0 & \\ 0 & 0 & 0 & 0 & p_{1,0,-1} & p_{1,0,0} & p_{1,0,1} & 0 & 0 & 0 \\ 0 & 0 & 0 & 0 & 0 & 0 & 0 & p_{1,1,-1} & p_{1,1,0} & p_{1,1,1} \end{array}\right] \end{array},$$

where the probabilities p_{i_{t-2},i_{t-1},i_t} denote the transition probabilities $p_{(i_{t-2},i_{t-1}),(i_{t-1},i_t)}$ which can be obtained from (1)−(6).

With the various values of ϕ_1, ϕ_2 and ξ, Tables 3.5 and 3.6 give numerical results for the ARLs in the $\mathrm{AR}^{\mathrm{II}}(2)$ process and results for the $\mathrm{AR}^{\mathrm{I}}(2)$ process are provided in Tables 3.7 and 3.8.

3.3 Average run lengths for AR(1) process with Western Electric rules

It is known that the Shewhart control chart is insensitive to small shifts in the process parameters. To enhance the ability for the chart to detect small shifts more quickly, one way is to add sensitive rules in the chart. Several frequently used rules that were suggested by the Western Electric Company (1956) are:

Rule 1 One or more points fall outside the three sigma control limits;

Rule 2 Two of three consecutive points fall outside the two-sigma warning limits;

Rule 3 Four of five consecutive points fall beyond the 1-sigma limits;

Rule 4 Eight points in a row fall on one side of the center line.

The above rules are always referred to *runs* rules. In the sequel, a control chart that uses several rules simultaneously is referred to a *compound control chart*. It should be noted that Rule 1 is included in all compound control charts. Also note that those rules can only be applied to one side of the center line. For example, if there are two consecutive points, one is plotted above the upper warning limit and the other is plotted below the lower warning limit, then Rule 2 is not applicable under this situation. In the successive sections, we study run-length properties for compound control charts that use two rules simultaneously in an AR(1) process. For convenience, we use the notation R_{1i} to denote the combinations of Rule 1 and Rule i for $i = 2, 3, 4$. We shall demonstrate that the discretization and imbedding procedures can be easily applied to these charts.

3.3.1 Compound control charts R_{12}

Assume first that the observations are from an $\mathrm{AR}^{\mathrm{I}}(1)$ process.

Step 1: Discretization

We have seen how the procedure of discretization works in Section 3.1. According to Rule 2, the chart is divided into four regions, say r_1, r_2, r_3 and r_4, by the control limits ($\pm h$) and the warming limits ($\pm h_w = \pm m_w \Delta$ where $m_w = \frac{2(m+1)}{3}$). For $t \geq 0$, we define

$$R(X_t) = \begin{cases} r_1 & \text{if } -h_w < D(X_t) < h_w, \\ r_2 & \text{if } h_w \leq D(X_t) < h, \\ r_3 & \text{if } -h < D(X_t) \leq -h_w, \\ r_4 & \text{otherwise.} \end{cases} \tag{3.10}$$

An illustration for these regions is shown in Figure 3.1.

Step 2: Imbedding

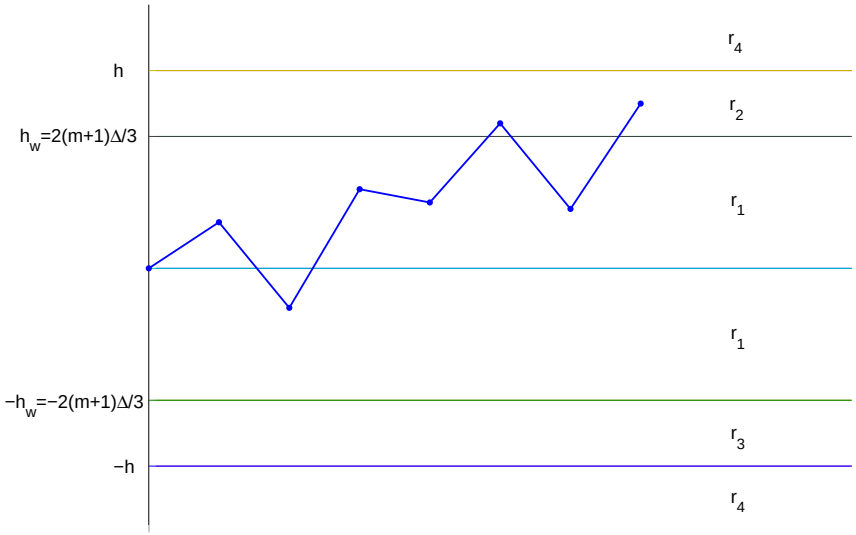

Figure 3.1: The regions based on the chart R_{12}.

Similar to the Step 2 in Section 3.2, we introduce two dummy variables X_{-1} and X_{-2} and define $R(X_{-1}) = R(X_{-2}) = \emptyset$ with $P(R(X_{-1}) = R(X_{-2}) = \emptyset) = 1$. We define a state space Ω by

$$\begin{aligned}\Omega \quad = \quad & \{(\emptyset,\emptyset),(\emptyset,-m),\ldots,(\emptyset,m),(r_1,-m),\ldots,(r_1,m),(r_2,-m),\ldots,(r_2,m_w-1),\\ & (r_3,-m_w+1),\ldots,(r_3,m),\alpha\}. \qquad (3.11)\end{aligned}$$

with $\text{card}(\Omega) = 6m + 2m_w + 3$. Note that the states are viewed as the absorbing state α if one of their components includes r_4 or $\pm(m+1)$. Base on the rules, we define a Markov chain $\{Y_t(m; R_{12})\}$ for $t \geq -1$ on the state space Ω as

$$Y_t(m; R_{12}) = [R(X_{t-1}), D(X_t)]. \qquad (3.12)$$

The imbedded Markov chain does not move into the absorbing state α at time $t+1$ if one of the following conditions holds:

(1) $-h_w < D(X_{t+1}) < h_w$,

(2) $h_w \leq D(X_{t+1}) < h$, $R(X_{t-1}) = \emptyset$ and $R(X_t) = \emptyset$ or r_1 or r_3,

(3) $-h < D(X_{t+1}) \leq -h_w$, $R(X_{t-1}) = \emptyset$ and $R(X_t) = \emptyset$ or r_1 or r_3,

(4) $h_w \leq D(X_{t+1}) < h$, $R(X_{t-1}) = r_1$ and $R(X_t) = r_1$ or r_3,

(5) $h_w \leq D(X_{t+1}) < h$ and $R(X_{t-1}) = R(X_t) = r_3$,

(6) $-h < D(X_{t+1}) \leq -h_w$, $R(X_{t-1}) = r_1$ and $R(X_t) = r_1$ or r_3,

(7) $-h < D(X_{t+1}) \leq -h_w$ and $R(X_{t-1}) = R(X_t) = r_3$.

It follows from (3.11) and (3.12) that the transition probabilities of the imbedded Markov chain from state (x, i) to state (y, j) can be determined by the following equations: if conditions (1)−(7) hold,

$$\begin{aligned}
&P(Y_{t+1}(m; R_{12}) = [R(X_t), D(X_{t+1})] \mid Y_t(m; R_{12}) = [R(X_{t-1}), D(X_t)]) \\
&= P(Y_{t+1}(m; R_{12}) = (y, j) \mid Y_t(m; R_{12}) = (x, i)) \\
&= \begin{cases} P((j - 0.5)\Delta \leq X_0 \leq (j + 0.5)\Delta) & \text{if } t = -1, \\ P((j - \phi i - 0.5)\Delta \leq \varepsilon_t \leq (j - \phi i + 0.5)\Delta) & \text{if } t \geq 0. \end{cases}
\end{aligned} \tag{3.13}$$

where $X_0 \sim N\left(0, \frac{1}{1-\phi^2}\right)$ and $\varepsilon_t \sim N(0, 1)$. Since the transition probabilities of each row add to 1, the probability of moving into the absorbing state α can be obtain by subtracting all the other probabilities in the row from 1: i.e.,

$$\begin{aligned}
&P(Y_{t+1}(m; R_{12}) = \alpha \mid Y_t(m; R_{12}) = (x, i)) \\
&= 1 - \sum_{(y,j) \in \Omega \setminus \{\alpha\}} P(Y_{t+1}(m; R_{12}) = (y, j) \mid Y_t = (x, i)).
\end{aligned} \tag{3.14}$$

For the case of $\mathrm{AR}^{\mathrm{II}}(1)$ model, we only need to define a variable $R(X_{-1}) = \emptyset$ with $P = (R(X_{-1}) = \emptyset) = 1$. With a simple modification in (3.11), the state space Ω is given by

$$\begin{aligned}
\Omega \;=\; &\{(\emptyset, 0), (r_1, -m), \ldots, (r_1, m), (r_2, -m), \ldots, (r_2, m_w - 1), \\
&(r_3, -m_w + 1), \ldots, (r_3, m)\}.
\end{aligned} \tag{3.15}$$

Example 3.3 Consider a compound control chart R_{12} in the $\mathrm{AR}^{\mathrm{II}}(1)$ process. Suppose we take m=2, then the state space of the imbedded Markov chain $\{Y_t(2; R_{12})\}$ is given by

$$\Omega = \{(\emptyset, 0), (r_1, -2), \ldots, (r_1, 2), (r_2, -2), \ldots, (r_2, 1), (r_3, -1), \ldots, (r_3, 2)\}.$$

The submatrix $\boldsymbol{N}(2)$ of the transition matrix $\boldsymbol{M}(2)$ is shown in the next page. Some numerical results of the ARLs are listed in Table 3.9.

3.3.2 Compound control charts R_{13}

Assume that the observations are from an $\mathrm{AR}^{\mathrm{I}}(1)$ process.

Step 1: Discretization

Similar to Section 3.3.1, we divide the chart into four regions, say r_1, r_2, r_3 and r_4 according to Rule 3. Note that the warning limits here are $\pm h_w = \pm m_w \Delta$ where $m_w = \frac{(m+1)}{3}$ (see Figure 3.2 for illustration). Define

$$R(X_t) = \begin{cases} r_1 & \text{if } -h_w < D(X_t) < h_w, \\ r_2 & \text{if } h_w \leq D(X_t) < h, \\ r_3 & \text{if } -h < D(X_t) \leq -h_w, \\ r_4 & \text{otherwise.} \end{cases} \tag{3.16}$$

Step 2: Imbedding

We introduce four dummy variable $X_{-1}, X_{-2}, X_{-3}, X_{-4}$ and define $R(X_{-4}) = R(X_{-3}) = R(X_{-2}) = R(X_{-1}) = \emptyset$ with probability one. Define a state space Ω by

$$\begin{aligned} \Omega \;=\; & \{(\emptyset, \emptyset, \emptyset, \emptyset), (\emptyset, \emptyset, \emptyset, i_1), (\emptyset, \emptyset, \mathcal{R}_1, i_2), (\emptyset, \mathcal{R}_2, \mathcal{R}_3, i_3), \\ & (\mathcal{R}_4, \mathcal{R}_5, \mathcal{R}_6, i_4), \alpha\}. \end{aligned}$$

where $\mathcal{R}_1, \mathcal{R}_2, \mathcal{R}_3, \mathcal{R}_4, \mathcal{R}_5, \mathcal{R}_6 = r_1, r_2, r_3$ and $i_1, i_2, i_3, i_4 = -m, \ldots, m$. Note that states are incorporated into an absorbing state α if one of the first three components includes r_4 or the last component includes $\pm(m+1)$. Based on the Rules 1 and 3, we define a Markov chain $\{Y_t(m; R_{13})\}$ on the state space Ω as, for $t \geq -1$,

$$Y_t(m; R_{13}) = [R(X_{t-3}), R(X_{t-2}), R(X_{t-1}), D(X_t)].$$

$$
\boldsymbol{N}(3)=
\begin{array}{c}
\\
(\emptyset,\emptyset)\\
(\emptyset,-2)\\
(\emptyset,-1)\\
(\emptyset,0)\\
(\emptyset,1)\\
(\emptyset,2)\\
(r_1,-2)\\
(r_1,-1)\\
(r_1,0)\\
(r_1,1)\\
(r_1,2)\\
(r_2,-2)\\
(r_2,-1)\\
(r_2,0)\\
(r_2,1)\\
(r_3,-1)\\
(r_3,0)\\
(r_3,1)\\
(r_3,2)
\end{array}
\begin{bmatrix}
0 & p_{-2} & p_{-1} & p_0 & p_1 & p_2 & 0 & 0 & 0 & 0 & 0 & 0 & 0 & 0 & 0 & 0 & 0 & 0 & 0\\
0 & 0 & 0 & 0 & 0 & 0 & 0 & 0 & 0 & 0 & 0 & 0 & 0 & 0 & 0 & p_{-2,-2} & p_{-2,-1} & p_{-2,0} & p_{-2,1}\\
0 & 0 & 0 & 0 & 0 & 0 & p_{-1,-2} & p_{-1,-1} & p_{-1,0} & p_{-1,1} & p_{-1,2} & 0 & 0 & 0 & 0 & 0 & 0 & 0 & 0\\
0 & 0 & 0 & 0 & 0 & 0 & p_{0,-2} & p_{0,-1} & p_{0,0} & p_{0,1} & p_{0,2} & 0 & 0 & 0 & 0 & 0 & 0 & 0 & 0\\
0 & 0 & 0 & 0 & 0 & 0 & p_{1,-2} & p_{1,-1} & p_{1,0} & p_{1,1} & p_{1,2} & 0 & 0 & 0 & 0 & 0 & 0 & 0 & 0\\
0 & 0 & 0 & 0 & 0 & 0 & 0 & 0 & 0 & 0 & 0 & p_{2,-2} & p_{2,-1} & p_{2,0} & p_{2,1} & 0 & 0 & 0 & 0\\
0 & 0 & 0 & 0 & 0 & 0 & 0 & 0 & 0 & 0 & 0 & 0 & 0 & 0 & 0 & p_{-2,-1} & p_{-2,0} & p_{-2,1} & p_{-2,2}\\
0 & 0 & 0 & 0 & 0 & 0 & p_{-1,-2} & p_{-1,-1} & p_{-1,0} & p_{-1,1} & p_{-1,2} & 0 & 0 & 0 & 0 & 0 & 0 & 0 & 0\\
0 & 0 & 0 & 0 & 0 & 0 & p_{0,-2} & p_{0,-1} & p_{0,0} & p_{0,1} & p_{0,2} & 0 & 0 & 0 & 0 & 0 & 0 & 0 & 0\\
0 & 0 & 0 & 0 & 0 & 0 & p_{1,-2} & p_{1,-1} & p_{1,0} & p_{1,1} & p_{1,2} & 0 & 0 & 0 & 0 & 0 & 0 & 0 & 0\\
0 & 0 & 0 & 0 & 0 & 0 & 0 & 0 & 0 & 0 & 0 & p_{2,-2} & p_{2,-1} & p_{2,0} & p_{2,1} & 0 & 0 & 0 & 0\\
0 & 0 & 0 & 0 & 0 & 0 & 0 & 0 & 0 & 0 & 0 & 0 & 0 & 0 & 0 & 0 & p_{-2,-1} & p_{-2,0} & p_{-2,1}\\
0 & 0 & 0 & 0 & 0 & 0 & p_{-1,-2} & p_{-1,-1} & p_{-1,0} & p_{-1,1} & p_{-1,2} & 0 & 0 & 0 & 0 & 0 & 0 & 0 & 0\\
0 & 0 & 0 & 0 & 0 & 0 & p_{0,-2} & p_{0,-1} & p_{0,0} & p_{0,1} & p_{0,2} & 0 & 0 & 0 & 0 & 0 & 0 & 0 & 0\\
0 & 0 & 0 & 0 & 0 & 0 & p_{1,-2} & p_{1,-1} & p_{1,0} & p_{1,1} & p_{1,2} & 0 & 0 & 0 & 0 & 0 & 0 & 0 & 0\\
0 & 0 & 0 & 0 & 0 & 0 & 0 & p_{-1,-1} & p_{-1,0} & p_{-1,1} & p_{-1,2} & 0 & 0 & 0 & 0 & 0 & 0 & 0 & 0\\
0 & 0 & 0 & 0 & 0 & 0 & 0 & p_{0,-1} & p_{0,0} & p_{0,1} & p_{0,2} & 0 & 0 & 0 & 0 & 0 & 0 & 0 & 0\\
0 & 0 & 0 & 0 & 0 & 0 & 0 & p_{1,-1} & p_{1,0} & p_{1,1} & p_{1,2} & 0 & 0 & 0 & 0 & 0 & 0 & 0 & 0\\
0 & 0 & 0 & 0 & 0 & 0 & 0 & 0 & 0 & 0 & 0 & 0 & p_{2,-1} & p_{2,0} & p_{2,1} & 0 & 0 & 0 & 0
\end{bmatrix}
$$

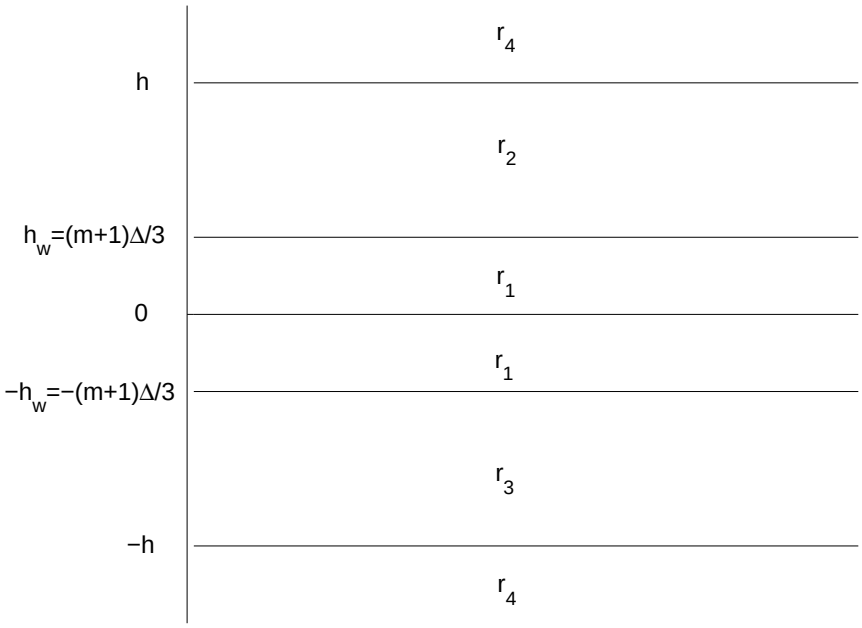

Figure 3.2: The regions based on the chart R_{13}.

To determine the transition probabilities, a set of conditions that the imbedded chain $\{Y_t(m; R_{13})\}$ does not move to α can be easily specified in a similar way as in Section 3.3.1. Finally, for the case of $\mathrm{AR}^{\mathrm{II}}(1)$ process, all the procedures are the same as discussed in Section 3.3.1. Some numerical results are presented in Table 3.10.

3.3.3 Compound control charts R_{14}

Step 1: Discretization

According to Rule 4, the chart can be divided into three regions (see Figure 3.3). We define

$$R(X_t) = \begin{cases} r^+ & \text{if } 0 < D(X_t) < h, \\ r^0 & \text{if } D(X_t) = 0, \\ r^- & \text{if } -h < D(X_t) < 0. \end{cases} \tag{3.17}$$

Step 2: Imbedding

We define a variable $C(X_t)$ to be the number of consecutive points that fall into the same regions r^+ or r^-. Then $C(X_t)$ could take values on $0, 1, \ldots, 8$. For $\mathrm{AR}^{\mathrm{I}}(1)$ process, a dummy variable X_{-1} is introduced and we define $C(X_{-1}) = \emptyset$

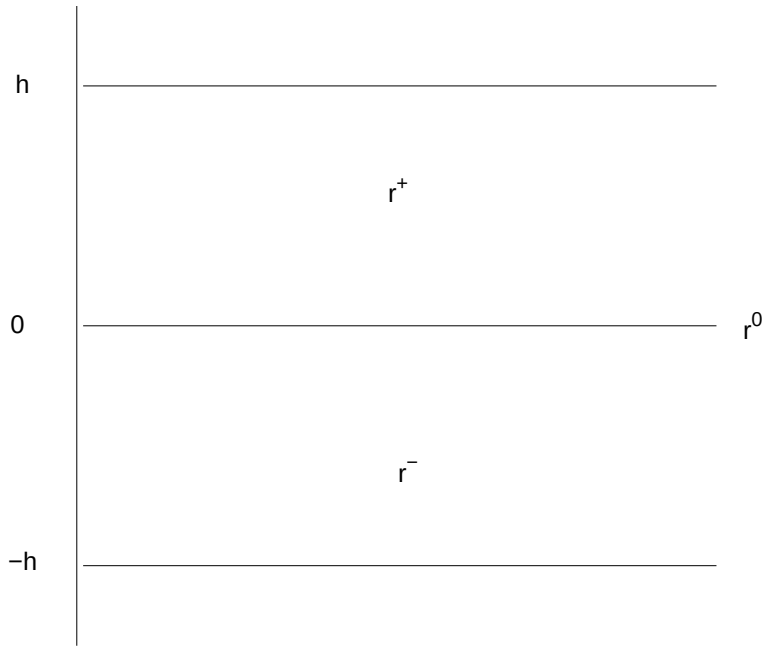

Figure 3.3: The regions based on Rule 4.

with probability one. Define a state space Ω by

$$\begin{aligned}\Omega &= \{(\emptyset,\emptyset),(0,0),(1,-m),\ldots,(1,-1),(1,1),\ldots,(1,m),(2,-m),\ldots,(2,-1),\\ &\quad (2,1),\ldots,(2,m),\ldots,(7,-m),\ldots,(7,-1),(7,1),\ldots,(7,m),\alpha\} \qquad (3.18)\end{aligned}$$

with $14m+3$ states in total. Note that states that include 8 in the first component or $\pm(m+1)$ in the second component are combined into an absorbing state α. For $t \geq -1$, we define a Markov chain $\{Y_t(m;R_{14})\}$ on the state space Ω by

$$Y_t(m;R_{14}) = [C(X_t), D(X_t)]. \qquad (3.19)$$

The transition probabilities can be specified by following the same procedure in Section 3.1.

Remark 3.1 For a continuous monitoring statistic, the region r^0 can be ignored since $P(D(X_t)=0) = P(-0.5\Delta \leq X_t \leq 0.5\Delta) \to 0$ as $m \to \infty$. Thus we can eliminate the state $(0,0)$ and modify the probabilities p_1 and p_{-1} in (3.3) as follows:

$$p_1 = \int_0^{1.5\Delta} f(x)\,dx,$$

$$p_{-1} = \int_{-1.5\Delta}^{0} f(x)\, dx. \tag{3.20}$$

If the monitoring statistic is discrete, then the region r^0 is needed and the state $(0, 0)$ should be retained.

Example 3.4 Consider a compound control chart R_{14} in an $\mathrm{AR}^{\mathrm{II}}(1)$ process. Take $m = 1$, then the state space is given by

$$\Omega = \{(\emptyset, \emptyset), (0,0), (1,-1), (1,0), (1,1), \ldots, (7,-1), (7,0), (7,1), \alpha\}.$$

The submatrix $\boldsymbol{N}(1)$ of $\boldsymbol{M}(1)$ is given in the next page. Table 3.11 gives some numerical results for the ARLs with various values of ϕ and ξ.

$$
\boldsymbol{N}(1)=
\begin{array}{r}
(\emptyset,\emptyset)\\
(0,0)\\
(1,-1)\\
(1,1)\\
(2,-1)\\
(2,1)\\
(3,-1)\\
(3,1)\\
(4,-1)\\
(4,1)\\
(5,-1)\\
(5,1)\\
(6,-1)\\
(6,1)\\
(7,-1)\\
(7,1)
\end{array}
\begin{bmatrix}
0 & p_{0} & p_{-1} & p_{1} & 0 & 0 & 0 & 0 & 0 & 0 & 0 & 0 & 0 & 0 & 0 & 0\\
0 & p_{0,0} & p_{0,-1} & p_{0,1} & 0 & 0 & 0 & 0 & 0 & 0 & 0 & 0 & 0 & 0 & 0 & 0\\
0 & p_{-1,0} & 0 & p_{-1,1} & p_{-1,-1} & 0 & 0 & 0 & 0 & 0 & 0 & 0 & 0 & 0 & 0 & 0\\
0 & p_{1,0} & p_{1,-1} & 0 & 0 & p_{1,1} & 0 & 0 & 0 & 0 & 0 & 0 & 0 & 0 & 0 & 0\\
0 & p_{-1,0} & 0 & p_{-1,1} & 0 & 0 & p_{-1,-1} & 0 & 0 & 0 & 0 & 0 & 0 & 0 & 0 & 0\\
0 & p_{1,0} & p_{1,-1} & 0 & 0 & 0 & 0 & p_{1,1} & 0 & 0 & 0 & 0 & 0 & 0 & 0 & 0\\
0 & p_{-1,0} & 0 & p_{-1,1} & 0 & 0 & 0 & 0 & p_{-1,-1} & 0 & 0 & 0 & 0 & 0 & 0 & 0\\
0 & p_{1,0} & p_{1,-1} & 0 & 0 & 0 & 0 & 0 & 0 & p_{1,1} & 0 & 0 & 0 & 0 & 0 & 0\\
0 & p_{-1,0} & 0 & p_{-1,1} & 0 & 0 & 0 & 0 & 0 & 0 & p_{-1,-1} & 0 & 0 & 0 & 0 & 0\\
0 & p_{1,0} & p_{1,-1} & 0 & 0 & 0 & 0 & 0 & 0 & 0 & 0 & p_{1,1} & 0 & 0 & 0 & 0\\
0 & p_{-1,0} & 0 & p_{-1,1} & 0 & 0 & 0 & 0 & 0 & 0 & 0 & 0 & p_{-1,-1} & 0 & 0 & 0\\
0 & p_{1,0} & p_{1,-1} & 0 & 0 & 0 & 0 & 0 & 0 & 0 & 0 & 0 & 0 & p_{1,1} & 0 & 0\\
0 & p_{-1,0} & 0 & p_{-1,1} & 0 & 0 & 0 & 0 & 0 & 0 & 0 & 0 & 0 & 0 & p_{-1,-1} & 0\\
0 & p_{1,0} & p_{1,-1} & 0 & 0 & 0 & 0 & 0 & 0 & 0 & 0 & 0 & 0 & 0 & 0 & p_{1,1}\\
0 & p_{-1,0} & 0 & p_{-1,1} & 0 & 0 & 0 & 0 & 0 & 0 & 0 & 0 & 0 & 0 & 0 & 0\\
0 & p_{1,0} & p_{1,-1} & 0 & 0 & 0 & 0 & 0 & 0 & 0 & 0 & 0 & 0 & 0 & 0 & 0
\end{bmatrix}
$$

Tables

Table 3.1: Convergence of means and standard deviations of $W(m)$ in Example 3.1 and Example 3.2 for various values of m.

	$h = 3$		$h = 3\sigma_x$	
m	ARL	SD	ARL	SD
3	109.83	108.43	338.58	337.57
12	118.88	117.49	394.41	393.13
30	119.29	117.91	396.98	395.80
100	119.36	117.97	397.42	396.24
300	119.36	117.98	397.46	396.28
1000	119.36	117.98	397.46	396.28

Table 3.2: Comparisons of the in-control ARLs for $h = 3$ and $h = 3\sigma_x$ in the $\mathrm{AR}^{\mathrm{II}}(1)$ process.

	$h = 3$		$h = 3\sigma_x$	
b	ARL	SD	ARL	SD
0	370.40	369.90	370.40	369.90
0.1	353.14	352.59	370.95	370.40
0.2	306.33	305.65	372.85	372.16
0.3	242.58	241.70	376.81	375.90
0.4	176.51	175.39	384.21	383.00
0.5	119.36	117.98	397.46	395.86
0.6	76.35	74.70	421.16	419.03
0.7	47.39	45.45	465.54	462.59
0.8	29.48	27.27	559.84	555.34
0.9	19.02	16.59	842.04	833.07

Table 3.3: ARLs for $AR^{I}(1)$ process with various combinations of ϕ and ξ.

ϕ	ξ	ARL	simulation	ϕ	ξ	ARL	simulation
0	0	370.40	371.24	0.5	0	396.28	398.01
	0.5	155.22	157.55		0.5	176.29	175.11
	1	43.89	44.43		1	54.35	54.16
	2	6.30	6.38		2	8.89	8.95
	3	2.00	1.98		3	2.57	2.59
0.1	0	370.90	370.02	0.6	0	419.37	422.34
	0.5	156.26	158.25		0.5	191.23	190.85
	1	44.64	44.42		1	60.65	61.15
	2	6.57	6.63		2	10.18	10.14
	3	2.07	2.08		3	2.84	2.82
0.2	0	372.65	372.96	0.7	0	462.78	460.50
	0.5	158.26	158.12		0.5	217.56	217.63
	1	45.83	45.92		1	71.31	71.71
	2	6.93	6.89		2	12.27	12.07
	3	2.15	2.18		3	3.25	3.23
0.3	0	376.38	379.23	0.8	0	555.16	551.18
	0.5	161.67	162.27		0.5	271.11	271.66
	1	47.63	48.42		1	92.39	91.80
	2	7.39	7.36		2	16.30	16.18
	3	2.26	2.24		3	4.05	4.05
0.4	0	383.46	385.62	0.9	0	831.67	827.44
	0.5	167.26	168.90		0.5	427.19	429.31
	1	50.31	49.88		1	152.99	150.80
	2	8.02	8.10		2	27.70	27.91
	3	2.39	2.40		3	6.26	6.12

Table 3.4: ARLs for $AR^{II}(1)$ process with various combinations of ϕ and ξ.

ϕ	ξ	ARL	simulation	ϕ	ξ	ARL	simulation
0	0	370.40	370.98	0.5	0	397.46	396.77
	0.5	155.22	157.94		0.5	177.27	177.95
	1	43.89	43.79		1	55.07	54.92
	2	6.30	6.37		2	9.14	9.05
	3	2.00	2.00		3	2.54	2.56
0.1	0	370.95	371.45	0.6	0	421.16	419.37
	0.5	156.30	156.55		0.5	192.75	194.98
	1	44.66	45.09		1	61.82	62.22
	2	6.58	6.65		2	10.60	10.68
	3	2.07	2.08		3	2.75	2.75
0.2	0	372.85	374.65	0.7	0	465.54	464.78
	0.5	158.40	158.18		0.5	219.95	217.22
	1	45.93	45.77		1	73.19	72.65
	2	6.96	6.88		2	12.99	13.15
	3	2.15	2.18		3	3.06	3.05
0.3	0	376.81	375.3812	0.8	0	559.84	555.1582
	0.5	162.00	161.73		0.5	275.19	279.34
	1	47.86	48.55		1	95.65	95.96
	2	7.47	7.39		2	17.62	17.70
	3	2.25	2.28		3	3.59	3.52
0.4	0	384.20	386.22	0.9	0	842.04	835.67
	0.5	167.86	168.28		0.5	436.26	438.18
	1	50.74	50.33		1	160.27	161.24
	2	8.16	8.09		2	30.73	30.69
	3	2.38	2.34		3	4.76	4.77

Table 3.5: ARLs for $AR^{II}(2)$ process with selected values of ϕ_1, ϕ_2 and ξ.

ϕ_1	ϕ_2	ξ	ARL	simulation	ϕ_1	ϕ_2	ξ	ARL	simulation
0	0	0	370.40	370.98	0.2	0	0	372.78	374.99
		0.5	155.22	155.35			0.5	158.39	159.49
		1	43.89	43.47			1	45.92	46.09
		2	6.30	6.22			2	6.96	6.96
		3	2.00	2.00			3	2.15	2.13
	0.2	0	372.97	376.49		0.2	0	378.87	380.06
		0.5	158.77	157.71			0.5	165.60	164.66
		1	46.43	46.30			1	50.57	50.41
		2	7.40	7.48			2	8.66	8.58
		3	2.35	2.31			3	2.64	2.64
	0.4	0	384.65	383.58		0.4	0	403.44	400.77
		0.5	168.81	171.24			0.5	186.42	183.88
		1	51.93	52.21			1	61.67	61.66
		2	9.13	9.14			2	11.97	12.14
		3	2.81	2.81			3	3.45	3.40
	0.6	0	421.96	419.40		0.5	0	436.11	515.19
		0.5	194.63	193.64			0.5	211.96	262.07
		1	64.12	64.01			1	75.94	97.53
		2	12.40	12.31			2	19.28	22.14
		3	3.48	3.52			3	9.20	5.56
	0.8	0	560.66	566.37		0.6	0	511.82	515.19
		0.5	279.11	279.52			0.5	261.90	262.07
		1	100.80	101.67			1	97.80	97.53
		2	21.60	21.26			2	22.01	22.14
		3	4.91	4.90			3	5.52	5.55

Table 3.6: Continuation of Table 3.5.

ϕ_1	ϕ_2	ξ	ARL	simulation	ϕ_1	ϕ_2	ξ	ARL	simulation
0.4	0	0	383.94	381.27	0.6	0	0	420.33	417.66
		0.5	167.78	167.16			0.5	192.51	195.31
		1	50.73	50.88			1	61.78	62.11
		2	8.16	8.24			2	10.60	10.47
		3	2.38	2.38			3	2.75	2.80
	0.2	0	409.48	417.16		0.1	0	457.40	460.60
		0.5	188.86	187.61			0.5	217.88	221.07
		1	61.84	61.2843			1	73.64	73.64
		2	11.47	11.41			2	13.75	13.54
		3	3.18	3.18			3	3.39	3.39
	0.4	0	529.53	530.80		0.2	0	544.59	542.03
		0.5	269.74	266.28			0.5	273.43	276.17
		1	99.44	99.73			1	98.37	96.91
		2	21.58	21.47			2	20.08	20.23
		3	5.26	5.18			3	4.58	4.53
	0.5	0	816.22	821.60		0.3	0	834.03	831.31
		0.5	447.30	449.20			0.5	448.65	454.45
		1	178.19	176.93			1	173.97	174.41
		2	42.82	42.49			2	39.34	39.13
		3	9.23	9.11			3	7.90	7.87

Table 3.7: ARLs for $AR^{I}(2)$ process with selected values of ϕ_1, ϕ_2 and ξ.

ϕ_1	ϕ_2	ξ	ARL	simulation	ϕ_1	ϕ_2	ξ	ARL	simulation
0	0	0	370.40	371.20	0.2	0	0	372.65	369.97
		0.5	155.22	156.03			0.5	158.26	160.76
		1	43.89	43.54			1	45.83	45.72
		2	6.30	6.21			2	6.93	6.92
		3	2.00	2.00			3	2.15	2.17
	0.2	0	372.64	372.42		0.2	0	378.23	379.13
		0.5	158.23	156.66			0.5	164.69	166.56
		1	45.78	46.04			1	49.56	49.05
		2	6.82	6.94			2	7.89	7.91
		3	2.08	2.08			3	2.32	2.32
	0.4	0	383.41	381.46		0.4	0	401.48	397.82
		0.5	167.16	166.25			0.5	183.78	182.93
		1	50.13	50.65			1	58.82	57.96
		2	7.71	7.62			2	9.86	9.75
		3	2.19	2.19			3	2.65	2.68
	0.6	0	419.17	415.13		0.5	0	432.97	429.73
		0.5	190.91	189.43			0.5	206.17	208.51
		1	60.13	59.44			1	68.83	69.01
		2	9.44	9.61			2	11.85	11.75
		3	2.39	2.39			3	2.99	3.00
	0.8	0	554.32	549.72		0.6	0	506.47	494.44
		0.5	269.92	269.89			0.5	254.58	252.95
		1	90.69	91.24			1	89.68	88.90
		2	14.25	14.41			2	15.89	15.77
		3	2.93	2.90			3	3.68	3.66

Table 3.8: Continuation of Table 3.7.

ϕ_1	ϕ_2	ξ	ARL	simulation	ϕ_1	ϕ_2	ξ	ARL	simulation
0.4	0	0	383.44	385.12	0.6	0	0	419.33	417.74
		0.5	167.25	167.77			0.5	191.22	189.91
		1	50.31	49.74			1	60.65	61.28
		2	8.02	8.06			2	10.18	10.14
		3	2.39	2.37			3	2.84	2.85
	0.2	0	407.94	405.53		0.1	0	455.56	451.66
		0.5	186.87	188.49			0.5	215.38	213.85
		1	59.80	60.77			1	71.15	71.46
		2	10.13	10.18			2	12.34	12.50
		3	2.78	2.79			3	3.24	3.27
	0.4	0	524.96	419.00		0.2	0	541.2812	547.48
		0.5	263.56	265.45			0.5	268.67	269.71
		1	92.73	91.72			1	93.32	93.14
		2	16.67	16.72			2	16.70	16.47
		3	3.97	3.85			3	4.07	4.05
	0.5	0	807.43	810.98		0.3	0	828.27	834.77
		0.5	433.77	431.85			0.5	438.08	440.57
		1	162.69	164.36			1	161.75	161.70
		2	30.162	29.46			2	29.84	29.17
		3	6.46	6.40			3	6.54	6.49

Table 3.9: ARLs for the compound control chart R_{12} in the $\mathrm{AR}^{\mathrm{II}}(1)$ process.

ϕ_1	ξ	ARL	simulation	ϕ_1	ξ	ARL	simulation
0	0	225.08	224.83	0.5	0	113.96	115.01
	0.5	77.59	77.44		0.5	56.90	56.22
	1	19.98	19.95		1	20.86	20.64
	2	3.64	3.73		2	4.73	4.91
	3	1.68	1.80		3	1.84	1.98
0.1	0	200.71	200.01	0.6	0	102.26	102.68
	0.5	72.50	73.66		0.5	55.84	56.39
	1	19.77	19.93		1	22.14	22.40
	2	3.78	3.93		2	5.15	5.41
	3	1.70	1.81		3	1.87	2.06
0.2	0	174.76	173.29	0.7	0	95.70	96.88
	0.5	67.48	66.76		0.5	57.05	57.30
	1	19.69	19.82		1	24.48	24.68
	2	3.95	4.11		2	5.74	5.97
	3	1.74	1.85		3	1.89	2.08
0.3	0	150.65	152.07	0.8	0	97.05	97.70
	0.5	63.02	62.98		0.5	63.03	63.01
	1	19.80	19.56		1	29.27	29.18
	2	4.16	4.36		2	6.66	6.95
	3	1.77	1.88		3	1.87	2.10
0.4	0	130.17	131.65	0.9	0	121.60	122.20
	0.5	59.41	58.52		0.5	85.95	85.77
	1	20.15	20.25		1	43.26	43.11
	2	4.41	4.56		2	8.60	8.91
	3	1.81	1.95		3	1.72	2.06

Table 3.10: ARLs for the compound control chart R_{13} in the $\mathrm{AR}^{\Pi}(1)$ process.

ϕ_1	ξ	ARL	simulation	ϕ_1	ξ	ARL	simulation
0	0	166.09	165.59	0.5	0	46.99	48.95
	0.5	46.27	46.44		0.5	26.21	27.37
	1	12.68	12.63		1	11.89	12.32
	2	3.68	3.69		2	4.26	4.25
	3	1.88	1.90		3	2.09	2.11
0.1	0	130.14	131.43	0.6	0	37.65	38.74
	0.5	40.90	41.76		0.5	23.80	25.10
	1	12.43	12.51		1	11.88	12.36
	2	3.76	3.78		2	4.42	4.43
	3	1.92	1.92		3	2.13	2.13
0.2	0	100.64	102.59	0.7	0	31.32	32.55
	0.5	36.36	37.00		0.5	22.00	23.45
	1	12.23	12.39		1	11.99	12.54
	2	3.87	3.86		2	4.59	4.63
	3	1.96	1.96		3	2.17	2.17
0.3	0	77.51	78.11	0.8	0	27.95	29.26
	0.5	32.47	33.18		0.5	21.29	22.56
	1	12.08	12.35		1	12.39	13.08
	2	3.98	3.99		2	4.73	4.79
	3	2.00	2.02		3	2.19	2.18
0.4	0	59.97	62.11	0.9	0	29.72	30.35
	0.5	29.11	30.24		0.5	23.69	25.38
	1	11.96	12.09		1	13.81	14.64
	2	4.12	4.15		2	4.72	4.76
	3	2.05	2.02		3	2.18	2.16

Table 3.11: ARLs for the compound control chart R_{14} in the $\mathrm{AR}^{\mathrm{II}}(1)$ process.

ϕ_1	ξ	ARL	simulation	ϕ_1	ξ	ARL	simulation
0	0	152.73	154.38	0.5	0	40.04	39.42
	0.5	44.28	44.82		0.5	25.27	25.29
	1	14.58	14.57		1	13.37	13.41
	2	4.89	4.91		2	5.80	5.82
	3	1.99	2.01		3	2.43	2.45
0.1	0	120.70	122.58	0.6	0	30.16	30.34
	0.5	40.35	40.44		0.5	21.82	21.79
	1	14.41	14.31		1	12.99	13.12
	2	5.00	4.99		2	6.09	6.12
	3	2.06	2.07		3	2.56	2.54
0.2	0	93.24	94.29	0.7	0	22.96	22.87
	0.5	36.44	36.30		0.5	18.58	18.54
	1	14.21	14.13		1	12.49	12.58
	2	5.15	5.14		2	6.44	6.43
	3	2.13	2.12		3	2.70	2.68
0.3	0	70.86	71.02	0.8	0	17.85	17.82
	0.5	32.60	32.62		0.5	15.63	15.71
	1	13.96	13.90		1	11.75	11.77
	2	5.33	5.36		2	6.85	6.83
	3	2.22	2.20		3	2.85	2.83
0.4	0	53.35	52.90	0.9	0	14.38	14.42
	0.5	28.87	29.15		0.5	13.05	13.04
	1	13.69	13.63		1	10.55	10.59
	2	5.54	5.56		2	7.32	7.35
	3	2.31	2.29		3	3.00	3.01

Chapter 4

CUSUM and EWMA Control Charts for Autocorrelated Processes

In this chapter, we investigate the run-length properties for the CUSUM and EWMA control charts and enhancement of these charts including combining Shewhart chart with CUSUM and EWMA charts when observations are from AR(1) and AR(2) processes. In addition, the fast initial response (FIR) feature for the CUSUM chart is also discussed.

4.1 One-sided CUSUM control charts

4.1.1 Average run lengths for AR(1) process

CUSUM control chart was first introduced by Page (1954). It is useful in detecting small shifts in the process mean. For a two-sided CUSUM chart, the monitoring statistics are given by

$$S_t^U = \max\{0, S_{t-1}^U + X_t - (\mu_0 + k)\}, \tag{4.1}$$

$$S_t^L = \max\{0, S_{t-1}^L - X_t + (\mu_0 - k)\}, \tag{4.2}$$

for $t = 1, 2, \ldots$, where the starting value $S_0^U (S_0^L)$ is set to be the target value and the parameter k is called a *reference value*. The two monitoring statistics S_t^U and S_t^L are only used for detecting the upward and downward shifts, respectively.The chart produces an out of control signal if S_t^U or $S_t^L \geq h$ for some $h > 0$. Here, we only discuss the upper-sided CUSUM control chart.

Step 1: Discretization

Let $X_t' = X_t - k$, then (4.1) can be written as

$$S_t^U = \max\{0, S_{t-1}^U + X_t'\}. \tag{4.3}$$

We discretize X_t' into a discrete random variable (denoted by $D(X_t')$) that takes values on $\{-m, \ldots, m+1\}$. This results in a discrete monitoring statistic $D(S_t^U)$ for S_t^U and $D(S_t^U) = i$ for $i = 0, \ldots, m+1$. Define the probabilities $p_i \equiv P(D(X_t') = i)$ as follows: for $i = -m+1, \ldots, m$,

$$\begin{aligned} p_i &= \int_{(i-0.5)\Delta+k}^{(i+0.5)\Delta+k} f(x)\ dx,\ i = 0, \pm 1, \ldots, \pm m, \\ p_{m+1} &= \int_{[(m+1)-0.5]\Delta+k}^{\infty} f(x)\ dx, \text{ and} \\ p_{-m} &= \int_{-\infty}^{(-m+0.5)\Delta+k} f(x)\ dx, \end{aligned} \tag{4.4}$$

where $f(x)$ is the density function of X. Notice that the discretized random variable $D(X_t')$ does not take the value $-(m+1)$ since it will not produce any out of control signal for the chart.

Step 2: Imbedding

Since the starting value X_0 is assumed to be from $N\left(0, \frac{1}{1-\phi^2}\right)$ and hence it is reasonable to define a dummy variable $D(X_{-1}') = \emptyset$ with probability one. This implies that $P(D(S_{-1}^U) = \emptyset) = 1$. Define a state space as

$$\begin{aligned} \Omega \ = \ & \{(\emptyset, \emptyset), (0, -m), \ldots, (0, m), \ldots, (i, -m), \ldots, (i, m), \ldots, (m, -m), \ldots, \\ & (m, m), \alpha\}. \end{aligned} \tag{4.5}$$

States that includes $m+1$ are combined into an absorbing state α. Based on (4.3), we define a Markov chain $\{Y_t(m)\}$ that takes values on the state space Ω by

$$Y_t(m) = [D(S_t^U), D(X_t')]. \tag{4.6}$$

Note that the number of states in Ω can be reduced. To see this, suppose that $D(S_t^U) = 0$ and $D(S_{t-1}^U) = i$, for $i = 0, 1, \ldots, m$, then $D(X_t')$ can only take values on j, $j = -m, -m+1, \ldots, 0$, according to (4.3). Hence states $(0,1), \ldots, (0,m)$ can be eliminated. In general, if $S_t = i$ then $D(X_t')$ can only take values on j, $j = -m+i, \ldots, i$. After reduction, the state space Ω is given by

$$\begin{aligned} \Omega \ = \ & \{(\emptyset, \emptyset), (0, -m), \ldots, (0, 0), \ldots, (i, -m+i), \ldots, (i, i), \ldots, (m, 0), \ldots, \\ & (m, m), \alpha\}. \end{aligned} \tag{4.7}$$

To find the transition probability p_{uv} from a state $u = (i_s, i_x)$ to a state $v = (j_s, j_x)$, the following condition

$$j_s = \max\{0, i_s + j_x\} \tag{4.8}$$

must be satisfied according to (4.3) and (4.6). From (4.7) and (4.8), the transition probabilities for the imbedded Markov chain $\{Y_t(m)\}$ can be specified as follows: for $t = 0$, we have

(1) if $j_x = -m+1, \ldots, m$ and $i_s, i_x = \emptyset$, then

$$\begin{aligned} p_{uv} &= P(Y_0(m) = (j_s, j_x) \mid Y_{-1}(m) = (\emptyset, \emptyset)) \\ &= P((j_x - 0.5)\Delta \le X_0' \le (j_x + 0.5)\Delta) \\ &= P((j_x - 0.5)\Delta + k \le X_0 \le (j_x + 0.5)\Delta + k), \end{aligned}$$

(2) if $j_x = -m$ and $i_s, i_x = \emptyset$, then

$$\begin{aligned} p_{uv} &= P(Y_0(m) = (j_s, j_x) \mid Y_{-1}(m) = (\emptyset, \emptyset)) \\ &= P(X_0' \le (-m + 0.5)\Delta) \\ &= P(X_0 \le (-m + 0.5)\Delta + k), \end{aligned}$$

(3) if $v = \alpha$ and $i_s, i_x = \emptyset$, then

$$\begin{aligned} p_{uv} &= P(Y_0(m) = \alpha) \mid Y_{-1}(m) = (\emptyset, \emptyset)) \\ &= P(X_0' \ge ((m+1) - 0.5)\Delta) \\ &= P(X_0 \ge (m + 0.5)\Delta + k), \end{aligned}$$

where $\emptyset + i = i$ by convention and $X_0 \sim N\left(0, \frac{1}{1-\phi^2}\right)$, and for $t \ge 1$, we have

(4) if $i_x = -m, \ldots, m$ and $j_x = -m+1, \ldots, m$, then

$$\begin{aligned} p_{uv} &= P(Y_t(m) = (j_s, j_x) \mid Y_{t-1}(m) = (i_s, i_x)) \\ &= P((j_x - 0.5)\Delta \le X_t' \le (j_x + 0.5)\Delta \mid X_{t-1}' = i_x\Delta) \\ &= P((j_x - 0.5)\Delta + k \le X_t \le (j_x + 0.5)\Delta + k \mid X_{t-1} = i_x\Delta + k) \\ &= P((j_x - 0.5)\Delta + k \le \phi X_{t-1} + \varepsilon_t \le (j_x + 0.5)\Delta + k \mid X_{t-1} = i_x\Delta + k) \\ &= P((j_x - \phi i_x - 0.5)\Delta + (1-\phi)k \le \varepsilon_t \le (j_x - \phi i_x + 0.5)\Delta + (1-\phi)k), \end{aligned}$$

(5) if $i_x = -m, \ldots, m$ and $j_x = -m$, then

$$\begin{aligned} p_{uv} &= P(Y_t(m) = (j_s, j_x) \mid Y_{t-1}(m) = (i_s, i_x)) \\ &= P(X'_t \le (-m + 0.5)\Delta \mid X'_{t-1} = i_x\Delta) \\ &= P(X_t \le (-m + 0.5)\Delta + k \mid X_{t-1} = i_x\Delta + k) \\ &= P(\phi X_{t-1} + \varepsilon_t \le (-m + 0.5)\Delta + k \mid X_{t-1} = i_x\Delta + k) \\ &= P(\varepsilon_t \le (-m + 0.5 - \phi i_x)\Delta + (1 - \phi)k), \end{aligned}$$

(6) if $i_x = -m, \ldots, m$ and $j = \alpha$, then

$$\begin{aligned} p_{uv} &= P(Y_t(m) = (m + 1, m + 1) \mid Y_{t-1}(m) = (i_s, i_x)) \\ &= P(X'_t \ge (m + 1 - 0.5)\Delta \mid X'_{t-1} = i_x\Delta) \\ &= P(X_t \ge (m + 0.5)\Delta + k \mid X_{t-1} = i_x\Delta + k) \\ &= P(\phi X_{t-1} + \varepsilon_t \ge (m + 0.5)\Delta + k \mid X_{t-1} = i_x\Delta + k) \\ &= P(\varepsilon_t \ge (m + 0.5 - \phi i_x)\Delta + (1 - \phi)k), \end{aligned}$$

(7) if $u = \alpha$, $j_x = 0, \pm 1, \ldots, \pm m$ and $j_s = 0, \ldots, m$, then

$$p_{uv} = 0,$$

(8) if $u = \alpha$ and $v = \alpha$, then

$$p_{uv} = 1,$$

where Φ is the cumulative density function of the standard normal distribution. The transition matrix $\boldsymbol{M}(m)$ for $Y_t(m)$ can be obtained and written in the form given by (2.2) and the exact probability, mean and standard deviation of run length can be calculated by Theorem 2.1.

Next, we consider the $\mathrm{AR}^{\mathrm{II}}(1)$ process. In this case, the starting value X_0 is assumed to be zero and this implies that $S_0^U = 0$ with $P(S_0^U = 0) = 1$. The state space and transition probabilities can be constructed in a similar fashion as the case of $\mathrm{AR}^{\mathrm{I}}(1)$ process.

The performance of a one-side CUSUM control chart always depends on the choices of the parameters h and k. For appropriate choices of parameters, we often take $h = 5\sigma_x$ and $k = \frac{1}{2}\xi$ where $\xi = \mu_1\sigma_x$ is the shift from 0 to μ_1. For example, we set k to be $\frac{1}{2}\sigma_x$ and $\frac{1}{4}\sigma_x$ if we would like to detect $1\sigma_x$ and $\frac{1}{2}\sigma_x$ shifts more quickly.

In Tables 4.1 and 4.2, we give some numerical results of the ARLs for an upper-sided CUSUM control chart in the $\mathrm{AR^I}(1)$ and $\mathrm{AR^{II}}(1)$ processes, respectively. For $\mathrm{AR^I}(1)$ process, we see that with $\phi = 0$ the in-control ARL is 930.32 and the out-of-control ARL for one-sigma shift is 10.38. Further, with $\phi = 0.9$ these two values are $\mathrm{ARL}_0 = 73.40$ and $\mathrm{ARL}_1 = 16.72$, respectively. We can conclude that high correlation causes violent reduction of the values of ARL_0 and increase the values of ARL_1 so that it is more difficult to detect a shift for the chart.

4.1.2 Average run lengths for AR(2) process

This section will investigate the run-length properties of an one-sided CUSUM control chart when the observations of process are modeled as an $\mathrm{AR^I}(2)$ process. The two steps are shown in the following.

Step 1 : Discretization

This step is completely the same as the procedure described in the previous section except that the probabilities in Equations (4.4) are generated from $N\left(0, \frac{(1-\phi_2)}{(1+\phi_2)(1-\phi_2+\phi_1)(1-\phi_2-\phi_1}\right)$ instead of $N\left(0, \frac{1}{1-\phi^2}\right)$

Step 2: Imbedding

We introduce two dummy variables S^U_{-1} and S^U_{-2} and define $D(S^U_{-1}) = D(S^U_{-2}) = \emptyset$ with probability one so that this stage of S^U_0 can be taken into account when computing the ARL. Now define a state space Ω by

$$\begin{aligned}\Omega &= \{(\emptyset,\emptyset,\emptyset),(0,\emptyset,-m),\ldots,(0,\emptyset,0),\ldots,(i,\emptyset,-m+i),\ldots,(i,\emptyset,i),\\ &\quad \ldots,(m,\emptyset,0),\ldots,(m,\emptyset,m),(i,j,k),\alpha\}. \qquad (4.9)\end{aligned}$$

where $i = 0,1,\ldots,m+1$, $j = -m,-m+1,\ldots,m,m+1$, and $k = i,i+1,\ldots,-m+i$. Note that states that include $m+1$ as one of the coordinates are combined into the

absorbing state α. We define a Markov chain $\{Y_t(m)\}$ on the state space Ω as

$$Y_t(m) = [D(S_t^U), D(X'_{t-1}), D(X'_t)]. \tag{4.10}$$

Based on (4.9) and (4.10), the transition probabilities can be determined with similar procedures stated in Section 4.1.

For the case of $\mathrm{AR}^{\mathrm{II}}(2)$ process, it is readily that we only need to define $D(X_{-1}) = \emptyset$ with $P(D(X_{-1}) = \emptyset)$=1. Hence, the state space Ω can be defined by modifying (4.9) as

$$\Omega = \{(0, 0, \emptyset), (i, j, k), \alpha\}, \tag{4.11}$$

where $i = 0, 1, \ldots, m+1$, $j = -m, -m+1, \ldots, m, m+1$, and $k = i, i+1, \ldots, -m+i$. Table 4.3 and Table 4.4 show the numerical results of ARLs for an upper-sided CUSUM chart in the $\mathrm{AR}^{\mathrm{I}}(2)$ and $\mathrm{AR}^{\mathrm{II}}(2)$ processes, respectively. Again, high correlation has the same effects for the ARLs as in the case of AR(1) process.

4.2 Enhancement of CUSUM control charts

4.2.1 Combined Shewhart-CUSUM control chart

It is known that a CUSUM control chart is not effective in detecting large shifts as a Shewhart control chart. To improve for this, we can use the Shewhart control chart and CUSUM control chart simultaneously. More precisely, we add a Shewhart control limit into the CUSUM control chart. Note that, the Shewhart control limit should be less than the CUSUM control limit. To gain the run-length properties for a combined Shewhart-CUSUM chart, we follow the same procedures discussed in Section 4.1 with slight modifications. There are two ways to modify the procedures: (i) reconstruct the state space according to the new control limits, or (ii) retain the state space defined in (4.7) and modify the transition probabilities according to the new control limits. We provide details in the following. Again we first assume that the observations are from an $\mathrm{AR}^{\mathrm{I}}(1)$ process.

(i) Let h be the control limit of an upper-sided CUSUM control chart. The chart signals if $S_t^U \geq h$. Now, we add the Shewhart control limit, denoted by h_s ($h_s \leq h + k$), into the CUSUM chart. Then the combined Shewhart-CUSUM chart gives an out of control signal if $S_t^U \geq h$ or $X_t' \geq h_s - k$. In a single CUSUM control chart, states that include $m + 1$ are regarding as the absorbing state α. Since there are two control limits h and h_s in the combined Shewhart-CUSUM chart, the chart is said to be out of control if $D(S_t^U) \geq h$ $(= (m+1)\Delta)$ or $D(X_t') \geq h_s - k$ $(= m^*\Delta$, where $m^* = [\frac{h_s - k}{\Delta}])$. Thus states that include $m + 1$ in the first component or states that include m^* in the second component are combined into an absorbing state α. Based on the discussion, the state space in (4.7) is modified as follows:

$$\begin{aligned}\Omega &= \{(\emptyset, \emptyset), (0, -m), \ldots, (0, 0), \ldots, (i, -m + i), \ldots, (m^* - 1, m^* - 1), \\ &\quad (m^*, m^* - 1), \ldots, (m, 0), \ldots, (m, m^* - 1), \alpha\}. \end{aligned} \tag{4.12}$$

The transition probability matrix $\boldsymbol{M}(m)$ of the imbedded Markov chain defined on Ω can be easily obtained. Note that we choose h_s to be $h_s = 4\sigma_x$ if $h = 5\sigma_x$ and $h_s = 3.5\sigma_x$ if $h = 4\sigma_x$. We do not use the traditional Shewhart control limit $h_s = 3\sigma_x$ since it may produce too many false alarms. We further apply the same procedures to the case of $\mathrm{AR}^{\mathrm{I}}(2)$ process. The state space in (4.9) can be modified as

$$\begin{aligned}\Omega &= \{(\emptyset, \emptyset, \emptyset), (0, -m, \emptyset), \ldots, (0, 0, \emptyset), \ldots, (m^* - 1, -m + m^* - 1, \emptyset), \ldots, \\ &\quad (m^* - 1, m^* - 1, \emptyset), \ldots, (m, 0, \emptyset), \ldots, (m, m^* - 1, \emptyset), (i, j, k), \alpha\}, \end{aligned} \tag{4.13}$$

where $i = 0, \ldots, m,\ j = -m+i, \ldots, \min(i, m^*-1)$ and $k = -m, \ldots, 0, \ldots, m^*-1$. We can also obtain the state space for $\mathrm{AR}^{\mathrm{II}}(1)$ and $\mathrm{AR}^{\mathrm{II}}(2)$ processes in a similar fashion. We do not give further discussion.

(ii) We retain the state space given by (4.7) and modify the transition probabilities

p_{uv} from a state $u = (i_s, i_x)$ to a state $v = (j_s, j_x)$ in the following sense:

$$\begin{aligned} p_{uv} &= P(\min(h_s, (j_x - 0.5)\Delta) - \phi i_x \Delta + (1-\phi)k, \\ &\quad \min(h_s, (j_x + 0.5)\Delta) - \phi i_x \Delta + (1-\phi)k). \end{aligned} \tag{4.14}$$

For $\mathrm{AR}^{\mathrm{II}}(1)$, $\mathrm{AR}^{\mathrm{I}}(2)$ and $\mathrm{AR}^{\mathrm{II}}(2)$ processes, the same approach remains applicable.

Tables 4.5 and 4.6 give the ARLs for a combined Shewhart-CUSUM control chart with various combinations of ϕ and ξ for $\mathrm{AR}^{\mathrm{I}}(1)$ and $\mathrm{AR}^{\mathrm{II}}(1)$ processes, respectively.

4.2.2 FIR feature

The concept of Fast Initial Response (FIR) arises from that the process may be already out of control at the beginning. Under this situation, we usually give a non-zero initial value H_0 (called a head-start value) for the CUSUM chart so that a shift on the process mean can be detected more quickly. If the process is in a state of statistical control, the value of the monitoring statistic will drop quickly without any effect on the performance of the chart. Lucas and Crosier (1982) recommended a head-start value to be $H_0 = \frac{h}{2} = \frac{m+1}{2}\Delta$ (m should be odd). With the FIR feature, all the procedures described in Section 4.1 remain the same except that the transition probability from the initial state $(\emptyset, \emptyset)$ to a given state (j_s, j_x) needs to be modified. To see this, suppose that for a given state (j_s, j_x) we have (without the FIR feature)

$$P(Y_0(m) = (j_s, j_x) \mid Y_{-1}(m) = (\emptyset, \emptyset)) = p. \tag{4.15}$$

If FIR is considered, then it turns out that the chain will move from state $(\emptyset, \emptyset)$ to state $(j_s + \frac{m+1}{2}, j_x)$ with the same probability p, that is,

$$P\left(Y_0(m) = \left(j_s + \frac{m+1}{2}, j_x\right) \mid Y_{-1}(m) = (\emptyset, \emptyset)\right) = p. \tag{4.16}$$

In Tables 4.7 and 4.8, we show the ARLs for a CUSUM chart with FIR feature for $\mathrm{AR}^{\mathrm{I}}(1)$ and $\mathrm{AR}^{\mathrm{II}}(1)$ processes, respectively.

4.3 EWMA control charts

4.3.1 Average run lengths for AR(1) process

The EWMA control chart was first proposed by Roberts (1954). It has been demonstrated that EWMA charts perform well as CUSUM charts for detecting small shifts in the process mean. The EWMA monitoring statistic S_t is given by

$$S_t = \lambda X_t + (1-\lambda) S_{t-1}, \tag{4.17}$$

where $0 < \lambda \leq 1$ is a constant and σ_x^2 is the variance of X. Clearly, Shewhart control chart is a special case of the EWMA chart when $\lambda = 1$. It has been shown by Hunter (1986) that

$$\sigma_s^2 = V(S_t) = \frac{\lambda[1-(1-\lambda)^{2t}]}{2-\lambda}\sigma_x^2, \tag{4.18}$$

and an steady-state variance is given by $\sigma_s \approx \sqrt{\frac{\lambda}{2-\lambda}}\sigma_x$ as $t \to \infty$. Hence the EWMA control chart can be established with control limit $\pm\, h$ (usually $h = 3\sigma_s$). The chart signals an alarm if $|S_t| \geq h$. To analyze the run-length properties of a EWMA control chart for $\mathrm{AR}^{\mathrm{I}}(1)$ process, we follow the two steps as follows:

Step 1: Discretization

Let $\pm h$ be the control limits of a EWMA chart. Given a positive integer m, the control chart is discretized into $2m+1$ regions within the interval $(-h, h)$ plus one region that exceeds the control limits. Then we obtain a sequence of discretized random variables $\{D(S_t)\}$ of $\{S_t\}$, where $D(S_t)$ takes values on i, for $i = 0, \pm 1, \ldots, \pm(m+1)$. We define the conditional probabilities $p_{j|i} = P(D(S_t) = j \mid D(S_{t-1}) = i)$ from a state i to a state j as follows: for $i, j = 0, \pm 1, \ldots, \pm m$,

$$\begin{aligned}
p_{j|i} &= \int_{(j-(1-\lambda)i-0.5)\Delta\frac{1}{\lambda}}^{(j-(1-\lambda)i+0.5)\Delta\frac{1}{\lambda}} f(x)\, dx, \\
p_{(m+1)|i} &= \int_{(m+1-(1-\lambda)i-0.5)\Delta\frac{1}{\lambda}}^{\infty} f(x)\, dx, \\
p_{-(m+1)|i} &= \int_{-\infty}^{(-(m+1)-(1-\lambda)i+0.5)\Delta\frac{1}{\lambda}} f(x)\, dx, \\
p_{j|(m+1)} &= p_{(-m-1)j} = 0, \text{ and} \\
p_{(m+1)|(m+1)} &= p_{(-m-1),(-m-1)} = 1.
\end{aligned} \tag{4.19}$$

Step 2: Imbedding

We introduce two dummy variables S_{-1} and S_{-2} and define $D(S_{-1}) = D(S_{-2}) = \emptyset$ with $P(D(S_{-1}) = D(S_{-2}) = \emptyset) = 1$. Further, define a state space Ω by

$$\begin{aligned}\Omega &= \{(\emptyset,\emptyset),(\emptyset,-m),\ldots,(\emptyset,m),(-m,-m),\ldots(-m,m),\ldots,\\ &\quad (0,-m),\ldots,(0,m),\ldots,(m,-m),\ldots,(m,m),\alpha\}. \qquad (4.20)\end{aligned}$$

As before, states that includes $\pm(m+1)$ are incorporated into an absorbing state α. For $t \geq -1$, we define a Markov chain $\{Y_t(m)\}$ that takes values on the state space Ω as

$$Y_t(m) = [D(S_{t-1}), D(S_t)]. \qquad (4.21)$$

It follows from (4.20) and (4.21) that the transition probabilities from state (i_{t-2}, i_{t-1}) at time $t-1$ to state (i_{t-1}, i_t) at time t for the imbedded Markov chain $\{Y_t(m)\}$ can be determined as follows: for $t = 0$, we have

(1) if $u = (\emptyset,\emptyset)$, $v = (\emptyset, i_0)$ and $i_0 = 0, \pm 1, \ldots, \pm m$, then

$$\begin{aligned}p_{uv} &= P(Y_0(m) = v \mid Y_{-1}(m) = u)\\ &= P(Y_0(m) = (\emptyset, i_0) \mid Y_{-1}(m) = (\emptyset,\emptyset))\\ &= P(((i_0 - 0.5)\Delta/\lambda) \leq X_0 \leq ((i_0 + 0.5)\Delta/\lambda))\\ &= P(((i_0 - 0.5)\Delta/\lambda) \leq X_0 \leq ((i_0 + 0.5)\Delta/\lambda)),\end{aligned}$$

(2) if $u = (\emptyset,\emptyset)$ and $v = \alpha$, then

$$\begin{aligned}p_{uv} &= P(Y_0(m) = v \mid Y_{-1}(m) = u)\\ &= P(X_0 \geq ((m+1) - 0.5)\Delta/\lambda \text{ or } X_0 \leq (-(m+1) + 0.5)\Delta/\lambda)\\ &= P(X_0 \geq (m + 0.5)\Delta/\lambda) + P(X_0 \leq (-m - 0.5)\Delta/\lambda)\end{aligned}$$

where $X_0 \sim N\left(0, \frac{1}{1-\phi^2}\right)$, and for $t \geq 1$, we have

(3) if $u = (i_{t-2}, i_{t-1})$, $v = (i_{t-1}, i_t)$, $i_{t-2} = \emptyset, 0, \pm 1, \ldots, \pm m$, and $i_{t-1}, i_t = 0, \pm 1, \ldots, \pm m$, then

$$p_{uv} = P(Y_t(m) = v \mid Y_{t-1}(m) = u)$$

$$
\begin{aligned}
&= P(Y_t(m) = (i_{t-1}, i_t) \mid Y_{t-1}(m) = (i_{t-2}, i_{t-1})) \\
&= P([(i_t - (1-\lambda)i_{t-1} - 0.5)\Delta/\lambda] \le X_t \le [(i_t - (1-\lambda)i_{t-1} + 0.5)\Delta/\lambda] \mid \\
&\quad X_{t-1} = (i_{t-1} - (1-\lambda)i_{t-2})\Delta/\lambda) \\
&= P([(i_t - (1-\lambda)i_{t-1} - 0.5)\Delta/\lambda] \le \phi X_{t-1} + \varepsilon_t \le [(i_t - (1-\lambda)i_{t-1} + 0.5) \\
&\quad \Delta/\lambda] \mid X_{t-1} = (i_{t-1} - (1-\lambda)i_{t-2})\Delta/\lambda) \\
&= P([(i_t - (1-\lambda)i_{t-1} - 0.5)\Delta/\lambda - \phi(i_{t-1} - (1-\lambda)i_{t-2})\Delta/\lambda] \le \varepsilon_t \le \\
&\quad [(i_t - (1-\lambda)i_{t-1} + 0.5)\Delta/\lambda - \phi(i_{t-1} - (1-\lambda)i_{t-2})\Delta/\lambda]) \\
&= \Phi([(i_t - (1-\lambda)i_{t-1} + 0.5) - \phi(i_{t-1} - (1-\lambda)i_{t-2})]\Delta/\lambda) - \\
&\quad \Phi([(i_t - (1-\lambda)i_{t-1} - 0.5) - \phi(i_{t-1} - (1-\lambda)i_{t-2})]\Delta/\lambda),
\end{aligned}
$$

(4) if $u = (i_{t-2}, i_{t-1})$, $v = \alpha$, $i_{t-2} = \emptyset, 0, \pm 1, \ldots, \pm m$, and $i_{t-1} = 0, \pm 1, \ldots, \pm m$, then

$$
\begin{aligned}
p_{uv} &= P(Y_t(m) = v \mid Y_{t-1}(m) = u) \\
&= P(Y_t(m) = \alpha \mid Y_{t-1}(m) = (i_{t-2}, i_{t-1})) \\
&= P(X_t \ge ((m+1) - (1-\lambda)i_{t-1} - 0.5)\Delta/\lambda \text{ or } X_t \ge (-(m+1) \\
&\quad -(1-\lambda)i_{t-1} + 0.5)\Delta/\lambda \mid X_{t-1} = (i_{t-1} - (1-\lambda)i_{t-2})\Delta/\lambda) \\
&= P(\varepsilon_t \ge [(m + 0.5 - (1-\lambda)i_{t-1}) - \phi(i_{t-1} - (1-\lambda)i_{t-2})]\Delta/\lambda \text{ or} \\
&\quad \varepsilon_t \le [(-m - 0.5 - (1-\lambda)i_{t-1}) - \phi(i_{t-1} - (1-\lambda)i_{t-2})]\Delta/\lambda) \\
&= 1 - \Phi([(m + 0.5 - (1-\lambda)i_{t-1}) - \phi(i_{t-1} - (1-\lambda)i_{t-2})]\Delta/\lambda) \\
&\quad + \Phi((-m - 0.5 - (1-\lambda)i_{t-1}) - \phi(i_{t-1} - (1-\lambda)i_{t-2})]\Delta/\lambda),
\end{aligned}
$$

(5) if $v = (i_{t-1}, i_t)$ and $i_{t-1}, i_t = 0, \pm 1, \ldots, \pm m$, then

$$p_{\alpha v} = 0,$$

(6) $p_{\alpha\alpha} = 1$.

For AR$^{\text{II}}$(1) process, the dummy variable S_{-2} is not required. Hence, the state space Ω is given by

$$
\begin{aligned}
\Omega &= \{(\emptyset, 0), (-m, -m), \ldots (-m, m), \ldots, (0, -m), \ldots, (0, m), \ldots, \\
&\quad (m, -m), \ldots, (m, m), \alpha\}. \qquad (4.22)
\end{aligned}
$$

The choices of the parameters for the EWMA control chart always affect the performance of the chart. By appropriately choosing the parameters λ and h, we can obtain the desirable run-length properties for the EWMA charts. It has been found that small λ is contributive to detect small shifts and large λ is contributive to detect large shifts. For detecting small shifts, $\lambda = 0.1$ and 0.2 are popular choices. Some numerical results are presented in Tables 4.9−4.12.

4.3.2 Average run lengths for AR(2) process

In this section, we first assume that the observations are from a $\mathrm{AR}^{\mathrm{I}}(2)$ process.

Step 1: Discretization

This step is completely the same as the one discussed in Section 4.3.1 except that $X_t \sim N\left(0, \frac{(1-\phi_2)}{(1+\phi_2)(1-\phi_2+\phi_1)(1-\phi_2-\phi_1}\right)$ for each t.

Step 2: Imbedding

We introduce three dummy variables S_{-1}, S_{-2} and S_{-3} and define an initial state $(D(S_{-3}), D(S_{-2}), D(S_{-1})) = (\emptyset, \emptyset, \emptyset)$ with probability one. Now define a state space Ω by

$$\Omega = \{(\emptyset, \emptyset, \emptyset), (\emptyset, i_1, i_2), (i_3, i_4, i_5), \alpha\}, \tag{4.23}$$

where $i_1 = \emptyset, 0, \pm 1, \ldots, \pm m$ and $i_2, i_3, i_4, i_5 = 0, \pm 1, \ldots, \pm m$. Note that states including the values $\pm(m+1)$ are combined into an absorbing state α. We define a Markov chain $\{Y_t(m)\}$ that takes values on the state space Ω by

$$Y_t(m) = [D(S_{t-2}), D(S_{t-1}), D(S_t)]. \tag{4.24}$$

Following the same procedure stated in Section 4.3.1, the transition probabilities can be easily obtained. We do not provide any further details.

4.4 Combined Shewhart-EWMA control chart

As the combined Shewhart-CUSUM chart, the combined Shewhart-EWMA control chart can enhance the ability for detecting large shifts. Let h_s and $-h_s$ be the

upper and lower control limits for a Shewhart control chart in the $AR^{I}(1)$ process. Let (i_{t-1}, i_t) be a state for the imbedded Markov chain $\{Y_t(m)\}$ at time t, then the combined Shewhart-EWMA chart is said to be out of control if $i_{t-1}, i_t = \pm(m+1)$, or $S_U \geq h_s$ or $S_L \leq -h_s$ where $S_U = (i_t - (1-\lambda)i_{t-1} + 0.5)\Delta/\lambda$ and $S_L = (i_t - (1-\lambda)i_{t-1} - 0.5)\Delta/\lambda$. The transition probability from a state $u = (i_{t-2}, i_{t-1})$ to a state $v = (i_{t-1}, i_t)$ in Section 4.3.1 is modified as

$$p_{uv} = P(\min\{h_s, \max(S_L, -h_s)\} - \phi(i_{t-1} - (1-\lambda)i_{t-2})\Delta/\lambda \leq \varepsilon_t \leq \max\{-h_s, \min(S_U, h_s)\} - \phi(i_{t-1} - (1-\lambda)i_{t-2})\Delta/\lambda). \quad (4.25)$$

For more details, see Lucas and Saccucci(1990) for the i.i.d. case.

Similarly, for AR(2) process the transition probability from a state $u = (i_{t-2}, i_{t-1}, i_t)$ to a state $v = (i_{t-1}, i_t, i_{t+1})$ should be modified according to the new contol limits as

$$\begin{aligned} p_{uv} \;=\; & P(\min\{h_s, \max(S'_L, -h_s)\} - \phi_1(i_t - (1-\lambda)i_{t-1}) \\ & -\phi_2(i_{t-1} - (1-\lambda)i_{t-2})\Delta/\lambda) \leq \varepsilon_t \leq \max\{-h_s, \min(S'_U, h_s)\} \\ & -(\phi_1(i_t - (1-\lambda)i_{t-1}) - \phi_2(i_{t-1} - (1-\lambda)i_{t-2})\Delta/\lambda)), \end{aligned} \quad (4.26)$$

where $S'_U = [i_{t+1} - (1-\lambda)i_t + 0.5]\Delta/\lambda$ and $S'_L = [i_{t+1} - (1-\lambda)i_t - 0.5]\Delta/\lambda$. Some numerical results are presented in Tables 4.13 $-$4.16.

Tables

Table 4.1: The ARLs of one-sided CUSUM chart for $AR^{I}(1)$ process with various combinations of ϕ and ξ.

ϕ	ξ	ARL	simulation	ϕ	ξ	ARL	simulation
0	0	930.32	932.52	0.5	0	105.53	105.56
	0.5	38.01	37.80		0.5	26.54	26.65
	1	10.38	10.25		1	11.17	11.05
	2	4.01	4.01		2	4.37	4.36
	3	2.57	2.57		3	2.69	2.70
0.1	0	494.55	492.34	0.6	0	84.93	84.64
	0.5	34.58	34.92		0.5	25.83	25.61
	1	10.46	10.54		1	11.58	11.52
	2	4.05	4.06		2	4.51	4.51
	3	2.59	2.60		3	2.73	2.71
0.2	0	296.59	299.11	0.7	0	72.64	72.58
	0.5	31.79	32.02		0.5	25.88	25.84
	1	10.57	10.55		1	12.26	12.23
	2	4.11	4.11		2	4.71	4.72
	3	2.61	2.62		3	2.78	2.78
0.3	0	195.49	194.11	0.8	0	67.29	67.43
	0.5	29.55	29.49		0.5	27.34	26.90
	1	10.71	10.68		1	13.53	13.60
	2	4.18	4.19		2	5.03	5.04
	3	2.64	2.63		3	2.84	2.84
0.4	0	139.06	139.27	0.9	0	73.40	73.76
	0.5	27.80	28.02		0.5	33.10	33.47
	1	10.90	10.74		1	16.72	16.74
	2	4.26	4.25		2	5.69	5.66
	3	2.66	2.67		3	2.95	2.98

Table 4.2: The ARLs of one-sided CUSUM chart for $AR^{II}(1)$ process with various combinations of ϕ and ξ.

ϕ	ξ	ARL	simulation	ϕ	ξ	ARL	simulation
0	0	930.32	933.24	0.5	0	105.98	106.23
	0.5	38.01	38.17		0.5	26.79	26.51
	1	10.38	10.38		1	11.29	11.29
	2	4.01	4.02		2	4.37	4.42
	3	2.57	2.57		3	2.67	2.67
0.1	0	494.56	495.82	0.6	0	85.67	86.65
	0.5	34.59	34.53		0.5	26.25	26.14
	1	10.47	10.56		1	11.77	11.86
	2	4.06	4.05		2	4.49	4.50
	3	2.59	2.58		3	2.68	2.68
0.2	0	296.65	297.31	0.7	0	73.86	72.76
	0.5	31.83	31.47		0.5	26.57	26.87
	1	10.58	10.46		1	12.54	12.61
	2	4.11	4.12		2	4.64	4.64
	3	2.61	2.61		3	2.68	2.69
0.3	0	195.63	195.32	0.8	0	69.40	70.90
	0.5	29.63	29.34		0.5	28.52	28.46
	1	10.743	10.76		1	13.91	13.98
	2	4.18	4.18		2	4.79	4.82
	3	2.63	2.63		3	2.65	2.66
0.4	0	139.33	137.72	0.9	0	77.86	76.71
	0.5	27.95	28.01		0.5	35.34	34.79
	1	10.96	11.02		1	16.99	17.09
	2	4.26	4.25		2	4.82	4.89
	3	2.65	2.66		3	2.57	2.56

Table 4.3: The ARLs of one-sided CUSUM chart for $AR^{I}(2)$ process with various combinations of ϕ_1, ϕ_2 and ξ.

ϕ_1	ϕ_2	ξ	ARL	simulation	ϕ_1	ϕ_2	ξ	ARL	simulation
0.2	0.1	0	203.00	202.51	0.5	0.1	0	85.91	88.06
		0.5	30.28	30.15			0.5	26.40	26.27
		1	10.86	10.95			1	11.82	11.77
		2	4.18	4.17			2	4.53	4.51
		3	2.63	2.63			3	2.73	2.72
	0.25	0	132.84	135.59		0.25	0	73.18	74.06
		0.5	28.96	28.81			0.5	28.18	28.28
		1	11.46	11.45			1	13.52	13.73
		2	4.32	4.33			2	4.92	4.89
		3	2.66	2.66			3	2.80	2.81
	0.45	0	92.96	93.29		0.4	0	84.28	85.52
		0.5	29.29	28.78			0.5	37.99	38.65
		1	12.87	12.71			1	18.78	18.78
		2	4.62	4.59			2	5.94	5.89
		3	2.71	2.71			3	2.96	2.93
	0.7	0	96.71	96.69	0.75	0.1	0	69.72	70.90
		0.5	42.00	42.71			0.5	30.15	30.16
		1	19.97	20.08			1	15.10	15.16
		2	5.91	5.91			2	5.34	5.32
		3	2.91	2.91			3	2.89	2.88
0.9	0.05	0	94.74	96.84		0.2	0	101.44	102.06
		0.5	44.59	44.77			0.5	47.59	47.59
		1	22.25	22.43			1	23.52	23.55
		2	6.65	6.52			2	6.81	6.86
		3	3.07	3.07			3	3.08	3.06

Table 4.4: The ARLs of one-sided CUSUM control chart for $AR^{II}(2)$ process with various combinations of ϕ and ξ.

ϕ_1	ϕ_2	ξ	ARL	simulation	ϕ_1	ϕ_2	ξ	ARL	simulation
0.2	0.1	0	203.17	202.73	0.5	0.1	0	86.73	86.87
		0.5	30.36	30.62			0.5	26.85	27.11
		1	10.90	11.03			1	11.99	11.96
		2	4.18	4.15			2	4.50	4.47
		3	2.62	2.64			3	2.67	2.67
	0.25	0	133.36	132.38		0.25	0	75.15	74.85
		0.5	29.21	29.17			0.5	29.21	29.39
		1	11.55	11.56			1	13.81	13.79
		2	4.31	4.32			2	4.71	4.66
		3	2.63	2.65			3	2.65	2.64
	0.45	0	94.49	94.96		0.4	0	90.15	91.00
		0.5	30.05	30.18			0.5	40.53	40.16
		1	13.08	13.08			1	18.55	18.37
		2	4.50	4.53			2	4.70	4.64
		3	2.63	2.63			3	2.55	2.55
	0.7	0	103.86	103.69	0.75	0.1	0	72.88	73.64
		0.5	44.82	44.52			0.5	31.80	31.76
		1	19.29	19.35			1	15.46	15.50
		2	4.51	4.48			2	4.84	4.80
		3	2.53	2.53			3	2.61	2.60
0.9	0.05	0	103.17	104.65		0.2	0	110.80	111.61
		0.5	47.97	48.21			0.5	51.04	51.70
		1	21.13	20.92			1	21.85	21.87
		2	4.52	4.53			2	4.46	4.42
		3	2.52	2.52			3	2.51	2.51

Table 4.5: The ARLs of combined Shewhart-CUSUM chart for $AR^{I}(1)$ process with various combinations of ϕ and ξ.

ϕ	ξ	ARL	simulation	ϕ	ξ	ARL	simulation
0	0	911.77	913.41	0.5	0	105.54	105.82
	0.5	37.93	38.10		0.5	26.54	26.35
	1	10.36	10.43		1	11.17	11.13
	2	3.96	3.94		2	4.34	4.37
	3	2.39	2.39		3	2.54	2.54
0.1	0	490.67	488.76	0.6	0	84.94	85.30
	0.5	34.54	35.08		0.5	25.83	25.93
	1	10.45	10.39		1	11.58	11.49
	2	4.01	4.02		2	4.48	4.47
	3	2.42	2.43		3	2.58	2.58
0.2	0	295.73	291.23	0.7	0	72.66	71.49
	0.5	31.77	31.87		0.5	25.88	25.67
	1	10.56	10.67		1	12.26	12.45
	2	4.07	4.07		2	4.69	4.69
	3	2.44	2.44		3	2.62	2.61
0.3	0	195.32	195.90	0.8	0	67.30	67.60
	0.5	29.54	29.71		0.5	27.34	27.41
	1	10.70	10.68		1	13.52	13.84
	2	4.14	4.12		2	5.00	5.00
	3	2.47	2.47		3	2.69	2.70
0.4	0	139.05	137.67	0.9	0	73.43	74.20
	0.5	27.80	27.85		0.5	33.11	33.92
	1	10.89	10.80		1	16.72	16.72
	2	4.23	4.20		2	5.66	5.62
	3	2.50	2.49		3	2.80	2.78

Table 4.6: The ARLs of combined Shewhart-CUSUM chart for $AR^{II}(1)$ process with various combinations of ϕ and ξ.

ϕ	ξ	ARL	simulation	ϕ	ξ	ARL	simulation
0	0	911.98	912.78	0.5	0	106.00	104.95
	0.5	37.93	38.11		0.5	26.79	27.07
	1	10.36	10.38		1	11.28	11.26
	2	3.96	3.97		2	4.35	4.39
	3	2.39	2.40		3	2.54	2.55
0.1	0	490.76	492.56	0.6	0	85.69	85.96
	0.5	34.54	34.29		0.5	26.25	26.08
	1	10.45	10.43		1	11.77	11.75
	2	4.01	4.01		2	4.48	4.48
	3	2.42	2.42		3	2.57	2.57
0.2	0	295.83	296.21	0.7	0	73.88	74.38
	0.5	31.80	32.26		0.5	26.58	26.40
	1	10.57	10.56		1	12.54	12.63
	2	4.08	4.07		2	4.63	4.64
	3	2.45	2.44		3	2.60	2.60
0.3	0	195.47	196.86	0.8	0	69.42	69.13
	0.5	29.62	29.35		0.5	28.52	29.00
	1	10.74	10.68		1	13.91	13.80
	2	4.15	4.16		2	4.79	4.77
	3	2.48	2.47		3	2.60	2.61
0.4	0	139.33	140.49	0.9	0	77.90	78.54
	0.5	27.94	28.00		0.5	35.35	35.22
	1	10.96	10.91		1	16.99	16.92
	2	4.24	4.27		2	4.82	4.81
	3	2.51	2.52		3	2.56	2.55

Table 4.7: The ARLs of CUSUM chart with FIR feature ($H_0 = \frac{h}{2}$) for AR$^{\text{I}}$(1) process with various combinations of ϕ and ξ.

ϕ	ξ	ARL	simulation	ϕ	ξ	ARLs	simulation
0	0	895.24	901.41	0.5	0	96.11	97.07
	0.5	28.70	28.48		0.5	20.98	20.74
	1	6.33	6.38		1	7.67	7.63
	2	2.36	2.38		2	2.66	2.69
	3	1.54	1.53		3	1.59	1.59
0.1	0	469.91	466.44	0.6	0	76.98	77.20
	0.5	26.29	26.22		0.5	20.71	20.87
	1	6.53	6.45		1	8.17	8.11
	2	2.40	2.42		2	2.77	2.81
	3	1.54	1.55		3	1.61	1.62
0.2	0	278.26	280.58	0.7	0	65.77	65.36
	0.5	24.36	24.46		0.5	21.10	21.18
	1	6.75	6.87		1	8.89	8.95
	2	2.45	2.46		2	2.93	2.92
	3	1.55	1.55		3	1.63	1.63
0.3	0	181.25	182.58	0.8	0	61.16	61.85
	0.5	22.85	22.93		0.5	22.77	22.50
	1	7.00	7.10		1	10.14	10.15
	2	2.51	2.53		2	3.17	3.17
	3	1.57	1.57		3	1.66	1.66
0.4	0	127.64	126.84	0.9	0	67.61	67.88
	0.5	21.72	21.52		0.5	28.49	28.24
	1	7.30	7.32		1	13.15	12.85
	2	2.58	2.62		2	3.68	3.77
	3	1.58	1.59		3	1.72	1.73

Table 4.8: The ARLs of CUSUM chart with FIR feature ($H_0 = \frac{h}{2}$) for $AR^{II}(1)$ process with various combinations of ϕ and ξ.

ϕ	ξ	ARL	simulation	ϕ	ξ	ARLs	simulation
0	0	895.24	890.21	0.5	0	97.41	96.58
	0.5	28.70	28.54		0.5	21.26	21.56
	1	6.33	6.38		1	7.69	7.70
	2	2.36	2.36		2	2.63	2.66
	3	1.54	1.54		3	1.56	1.56
0.1	0	470.04	474.56	0.6	0	78.72	78.83
	0.5	26.30	26.06		0.5	21.14	21.19
	1	6.53	6.52		1	8.17	8.27
	2	2.40	2.39		2	2.70	2.67
	3	1.54	1.55		3	1.56	1.57
0.2	0	278.65	274.94	0.7	0	68.17	67.67
	0.5	24.40	24.33		0.5	21.76	21.60
	1	6.75	6.80		1	8.86	8.89
	2	2.45	2.47		2	2.76	2.75
	3	1.55	1.55		3	1.55	1.55
0.3	0	181.91	183.51	0.8	0	64.73	64.88
	0.5	22.94	23.01		0.5	23.81	24.09
	1	7.01	7.01		1	9.96	10.03
	2	2.51	2.53		2	2.78	2.82
	3	1.56	1.56		3	1.52	1.53
0.4	0	128.60	129.66	0.9	0	74.11	73.70
	0.5	21.89	22.08		0.5	30.23	30.26
	1	7.31	7.48		1	12.12	12.03
	2	2.57	2.56		2	2.63	2.65
	3	1.56	1.57		3	1.50	1.51

Table 4.9: The ARLs of EWMA chart for $AR^{I}(1)$ process with λ=0.2 and various combinations of ϕ and ξ.

ϕ	ξ	ARL	simulation	ϕ	ξ	ARL	simulation
0	0	559.68	556.54	0.5	0	62.32	61.63
	0.5	44.13	43.97		0.5	28.22	28.04
	1	10.84	10.81		1	11.52	11.47
	2	3.8	3.83		2	4.21	4.21
	3	2.41	2.41		3	2.54	2.53
0.1	0	306.01	308.44	0.6	0	48.33	48.03
	0.5	39.18	39.02		0.5	26.67	26.68
	1	10.86	10.77		1	11.97	11.88
	2	3.85	3.84		2	4.37	4.39
	3	2.43	2.42		3	2.58	2.59
0.2	0	184.91	182.69	0.7	0	39.43	39.71
	0.5	35.43	35.84		0.5	25.55	25.41
	1	10.92	10.95		1	12.68	12.72
	2	3.92	3.93		2	4.59	4.54
	3	2.45	2.43		3	2.63	2.63
0.3	0	120.98	119.56	0.8	0	34.23	34.07
	0.5	32.49	32.49		0.5	25.22	25.02
	1	11.04	10.91		1	13.91	13.84
	2	3.99	4.00		2	4.96	4.94
	3	2.48	2.47		3	2.70	2.70
0.4	0	84.47	84.61	0.9	0	33.56	33.74
	0.5	30.14	30.44		0.5	27.29	27.26
	1	11.23	11.13		1	16.81	16.56
	2	4.09	4.07		2	5.75	5.81
	3	2.51	2.50		3	2.82	2.81

Table 4.10: The ARLs of EWMA chart for $AR^{I}(1)$ process with λ=0.1 and various combinations of ϕ and ξ.

ϕ	ξ	ARL	simulation	ϕ	ξ	ARL	simulation
0	0	841.46	847.33	0.5	0	76.99	77.04
	0.5	37.41	37.02		0.5	29.57	29.74
	1	11.38	11.49		1	12.29	12.44
	2	4.67	4.68		2	5.01	5.02
	3	3.05	3.04		3	3.16	3.17
0.1	0	437.58	434.22	0.6	0	57.20	57.29
	0.5	35.37	35.94		0.5	28.35	28.37
	1	11.48	11.46		1	12.72	12.81
	2	4.71	4.71		2	5.15	5.14
	3	3.06	3.07		3	3.20	3.22
0.2	0	254.20	252.25	0.7	0	44.32	44.27
	0.5	33.64	34.06		0.5	27.13	27.21
	1	11.60	11.58		1	13.38	13.52
	2	4.76	4.74		2	5.35	5.33
	3	3.08	3.08		3	3.25	3.26
0.3	0	160.63	161.02	0.8	0	36.07	36.44
	0.5	32.14	31.91		0.5	26.11	25.79
	1	11.76	11.82		1	14.44	14.43
	2	4.83	4.83		2	5.67	5.66
	3	3.10	3.09		3	3.31	3.33
0.4	0	108.34	110.02	0.9	0	32.04	31.71
	0.5	30.81	30.58		0.5	26.27	26.38
	1	11.98	11.82		1	16.59	16.78
	2	4.91	4.88		2	6.34	6.31
	3	3.13	3.13		3	3.43	3.41

Table 4.11: The ARLs of EWMA chart for$AR^{II}(1)$ process with λ=0.2 and various combinations of ϕ and ξ.

ϕ	ξ	ARL	simulation	ϕ	ξ	ARL	simulation
0	0	559.68	563.53	0.5	0	62.73	62.64
	0.5	44.13	44.01		0.5	28.41	28.10
	1	10.84	10.80		1	11.60	11.53
	2	3.8	3.80		2	4.21	4.21
	3	2.41	2.42		3	2.52	2.52
0.1	0	306.03	309.92	0.6	0	49.01	48.10
	0.5	39.19	39.23		0.5	27.03	27.11
	1	10.86	10.85		1	12.11	12.03
	2	3.85	3.86		2	4.36	4.36
	3	2.43	2.44		3	2.53	2.53
0.2	0	184.96	186.33	0.7	0	40.56	40.46
	0.5	35.44	36.29		0.5	26.23	26.14
	1	10.93	10.98		1	12.92	12.90
	2	3.92	3.93		2	4.54	4.54
	3	2.45	2.45		3	2.53	2.54
0.3	0	121.10	120.79	0.8	0	36.23	36.72
	0.5	32.54	32.05		0.5	26.51	26.72
	1	11.06	11.01		1	14.34	14.27
	2	3.99	3.99		2	4.78	4.76
	3	2.47	2.48		3	2.50	2.50
0.4	0	84.70	85.28	0.9	0	37.95	38.28
	0.5	30.24	30.98		0.5	30.30	30.49
	1	11.27	11.20		1	17.60	17.89
	2	4.09	4.08		2	4.98	4.95
	3	2.50	2.49		3	2.38	2.38

Table 4.12: The ARLs of EWMA chart for $AR^{\Pi}(1)$ process with λ=0.1 and various combinations of ϕ and ξ.

ϕ	ξ	ARL	simulation	ϕ	ξ	ARL	simulation
0	0	841.46	837.91	0.5	0	77.36	76.88
	0.5	37.41	37.52		0.5	29.70	29.47
	1	11.38	11.48		1	12.33	12.26
	2	4.67	4.68		2	5.01	5.01
	3	3.05	3.05		3	3.15	3.16
0.1	0	437.59	440.23	0.6	0	57.83	57.33
	0.5	35.37	35.20		0.5	28.61	28.90
	1	11.48	11.45		1	12.80	12.78
	2	4.71	4.71		2	5.14	5.13
	3	3.06	3.06		3	3.18	3.18
0.2	0	254.25	252.10	0.7	0	45.38	45.69
	0.5	33.64	33.37		0.5	27.66	27.85
	1	11.61	11.61		1	13.53	13.35
	2	4.76	4.76		2	5.31	5.27
	3	3.08	3.08		3	3.20	3.20
0.3	0	160.74	159.28	0.8	0	37.95	38.42
	0.5	32.16	32.22		0.5	27.20	27.21
	1	11.77	11.77		1	14.72	14.68
	2	4.83	4.84		2	5.51	5.53
	3	3.10	3.11		3	3.20	3.23
0.4	0	108.55	108.48	0.9	0	36.09	36.43
	0.5	30.87	31.26		0.5	28.88	28.52
	1	12.00	11.98		1	17.08	17.05
	2	4.91	4.93		2	5.66	5.63
	3	3.13	3.13		3	3.15	3.15

Table 4.13: The ARLs of combined Shewhart-EWMA chart for $AR^{I}(1)$ process with λ=0.2 and various combinations of ϕ and ξ.

ϕ	ξ	ARL	simulation	ϕ	ξ	ARL	simulation
0	0	546.77	548.35	0.5	0	62.31	62.88
	0.5	44.04	44.15		0.5	28.21	27.76
	1	10.82	10.81		1	11.52	11.50
	2	3.76	3.77		2	4.18	4.19
	3	2.26	2.26		3	2.40	2.38
0.1	0	302.93	302.10	0.6	0	48.33	47.71
	0.5	39.13	39.27		0.5	26.67	26.96
	1	10.85	10.82		1	11.97	12.00
	2	3.82	3.82		2	4.34	4.36
	3	2.28	2.30		3	2.44	2.44
0.2	0	184.11	183.01	0.7	0	39.43	39.64
	0.5	35.40	35.07		0.5	25.55	25.69
	1	10.92	10.87		1	12.68	12.51
	2	3.89	3.88		2	4.57	4.55
	3	2.31	2.31		3	2.49	2.49
0.3	0	120.77	120.69	0.8	0	34.23	34.27
	0.5	32.48	32.74		0.5	25.22	24.78
	1	11.04	10.94		1	13.91	13.96
	2	3.96	3.95		2	4.94	4.94
	3	2.34	2.34		3	2.56	2.58
0.4	0	84.42	84.23	0.9	0	33.56	33.29
	0.5	30.13	30.48		0.5	27.29	26.87
	1	11.23	11.27		1	16.81	16.76
	2	4.06	4.07		2	5.73	5.81
	3	2.37	2.38		3	2.68	2.67

Table 4.14: The ARLs of combined Shewhart-EWMA chart for $AR^{I}(1)$ process with λ=0.1 and various combinations of ϕ and ξ.

ϕ	ξ	ARL	simulation	ϕ	ξ	ARL	simulation
0	0	805.14	806.34	0.5	0	76.93	76.83
	0.5	37.33	37.22		0.5	29.56	29.83
	1	11.35	11.33		1	12.28	12.46
	2	4.58	4.59		2	4.97	4.95
	3	2.75	2.76		3	2.94	2.95
0.1	0	428.75	424.30	0.6	0	57.19	56.01
	0.5	35.31	35.31		0.5	28.35	28.54
	1	11.46	11.44		1	12.72	12.87
	2	4.63	4.65		2	5.11	5.12
	3	2.78	2.78		3	3.00	2.99
0.2	0	251.73	255.22	0.7	0	44.32	43.93
	0.5	33.59	33.76		0.5	27.13	26.98
	1	11.58	11.64		1	13.38	13.42
	2	4.69	4.66		2	5.32	5.30
	3	2.82	2.83		3	3.06	3.06
0.3	0	159.89	160.65	0.8	0	36.07	35.53
	0.5	32.11	32.18		0.5	26.11	26.21
	1	11.75	11.77		1	14.44	14.43
	2	4.76	4.77		2	5.65	5.56
	3	2.85	2.86		3	3.14	3.12
0.4	0	108.12	109.06	0.9	0	32.04	32.43
	0.5	30.79	30.63		0.5	26.27	26.02
	1	11.97	12.01		1	16.59	16.62
	2	4.85	4.84		2	6.31	6.33
	3	2.90	2.90		3	3.27	3.27

Table 4.15: The ARLs of combined Shewhart-EWMA chart for $AR^{II}(1)$ process with λ=0.2 and various combinations of ϕ and ξ.

ϕ	ξ	ARL	simulation	ϕ	ξ	ARL	simulation
0	0	546.77	550.61	0.5	0	62.72	62.89
	0.5	44.04	44.25		0.5	28.41	28.26
	1	10.82	10.84		1	11.60	11.71
	2	3.76	3.78		2	4.20	4.19
	3	2.26	2.26		3	2.40	2.40
0.1	0	302.95	305.09	0.6	0	49.01	48.75
	0.5	39.14	39.27		0.5	27.03	26.83
	1	10.85	10.90		1	12.11	12.19
	2	3.82	3.83		2	4.35	4.35
	3	2.28	2.28		3	2.43	2.44
0.2	0	184.16	183.36	0.7	0	40.56	40.65
	0.5	35.42	35.17		0.5	26.23	26.05
	1	10.92	10.90		1	12.92	12.92
	2	3.89	3.87		2	4.54	4.54
	3	2.31	2.32		3	2.46	2.45
0.3	0	120.90	121.29	0.8	0	36.23	36.45
	0.5	32.52	32.62		0.5	26.51	26.59
	1	11.05	11.11		1	14.34	14.23
	2	3.97	3.97		2	4.78	4.71
	3	2.34	2.34		3	2.45	2.45
0.4	0	84.65	84.79	0.9	0	37.95	37.97
	0.5	30.23	30.02		0.5	30.30	30.27
	1	11.27	11.30		1	17.60	17.78
	2	4.07	4.09		2	4.98	5.01
	3	2.37	2.37		3	2.37	2.38

Table 4.16: The ARLs of combined Shewhart-EWMA chart for $AR^{II}(1)$ process with λ=0.1 and various combinations of ϕ and ξ.

ϕ	ξ	ARL	simulation	ϕ	ξ	ARL	simulation
0	0	805.14	801.24	0.5	0	77.31	78.09
	0.5	37.33	37.20		0.5	29.69	29.53
	1	11.35	11.38		1	12.32	12.35
	2	4.58	4.57		2	4.99	4.99
	3	2.75	2.75		3	2.97	2.98
0.1	0	428.76	429.33	0.6	0	57.82	57.60
	0.5	35.31	35.30		0.5	28.61	28.45
	1	11.46	11.50		1	12.80	12.86
	2	4.63	4.62		2	5.13	5.13
	3	2.78	2.77		3	3.03	3.05
0.2	0	251.78	256.63	0.7	0	45.38	45.37
	0.5	33.60	33.89		0.5	27.66	27.77
	1	11.59	11.66		1	13.53	13.50
	2	4.70	4.69		2	5.30	5.28
	3	2.82	2.81		3	3.09	3.09
0.3	0	160.01	158.93	0.8	0	37.95	37.69
	0.5	32.13	32.38		0.5	27.20	27.10
	1	11.76	11.78		1	14.72	14.69
	2	4.77	4.76		2	5.51	5.54
	3	2.87	2.87		3	3.14	3.14
0.4	0	108.34	108.49	0.9	0	36.09	36.31
	0.5	30.85	30.79		0.5	28.88	28.88
	1	12.00	12.05		1	17.08	17.14
	2	4.87	4.85		2	5.66	5.66
	3	2.92	2.92		3	3.14	3.13

Chapter 5

Comparisons

In this chapter, we compare the performances of compound control charts $R_{1i},\ i = 2, 3, 4$, with EWMA and combined Shewhart-EWMA charts for $\mathrm{AR}^{\mathrm{I}}(1)$ process. For each chart, we set up the value of ARL_0 to be 250. In Table 5.1, we list numerical results of ARL_1 corresponding to different levels of shifts for compound control charts and EWMA charts with $\lambda = 0.2$ which is the most common used value. Table 5.2 shows numerical results of ARL_1 for compound and Shewhart-EWMA control charts with selected values of λ. At each level of shift, the smallest ARL_1 value is presented in a boldface style.

Some conclusions can be drawn from these numerical results. From Table 5.1, we see that compound control charts only have advantages for large shifts and for higher values of ϕ. Moreover, Table 5.2 asserts that for $\lambda = 0.1$ and 0.2, the combined Shewhart-EWMA charts perform better (except $\phi = 0.9$) than compound control charts when the the levels of shifts are less than or equal to two sigma. For larger shifts, the combined Shewhart-EWMA charts still perform better except for the values $\phi = 0.25$ and $\lambda = 0.7$ and 0.9. In general, we have found that the combined Shewhart-EWMA control charts perform well in most cases.

Table 5.1: Numerical values of ARLs for compound control and EWMA charts ($\lambda = 0.2$) for $AR^{I}(1)$ process.

ϕ	ξ	R_{12}	R_{13}	R_{14}	EWMA
0	0	250.41	249.91	250.06	249.55
	0.5	84.50	60.28	57.75	**29.99**
	1	21.26	14.91	18.43	**8.88**
	2	3.76	4.03	8.00	**3.39**
	3	**1.70**	2.08	4.54	2.21
0.25	0	250.59	250.15	N/A	250.27
	0.5	91.83	69.30	–	**45.24**
	1	25.40	19.24	–	**13.00**
	2	4.66	5.22	–	**4.37**
	3	**1.90**	2.85	–	2.65
0.5	0	250.16	250.27	N/A	250.09
	0.5	106.98	86.84	–	**68.70**
	1	33.69	27.25	–	**20.61**
	2	6.45	7.03	–	**6.03**
	3	**2.28**	4.06	–	3.33
0.75	0	250.38	250.36	N/A	250.50
	0.5	131.04	114.61	–	**108.51**
	1	49.27	43.07	–	**38.18**
	2	10.13	10.37	–	**9.88**
	3	**2.84**	4.82	–	4.56
0.9	0	250.11	249.48	N/A	250.53
	0.5	158.02	**146.87**	–	151.04
	1	71.15	**65.65**	–	66.15
	2	**14.82**	15.02	–	16.34
	3	**2.66**	4.92	–	5.78

N/A : The in-control ARLs can not reach 250.

Table 5.2: Numerical values of ARLs for compound control and Shewhart-EWMA charts for $AR^1(1)$ process.

ϕ	ξ	R_{12}	R_{13}	R_{14}	$S-E_{0.2}$	$S-E_{0.1}$	$S-E_{0.7}$	$S-E_{0.9}$
0	0	250.41	249.91	250.06	250.16	249.47	249.63	249.56
	0.5	84.50	60.28	57.75	30.12	**24.65**	74.49	97.61
	1	21.26	14.91	18.43	**8.89**	8.97	18.25	26.99
	2	3.76	4.03	8.00	**3.37**	3.89	3.51	4.43
	3	1.70	2.08	4.54	2.11	2.43	**1.68**	1.73
0.25	0	250.59	250.15	N/A	250.85	250.00	250.54	249.34
	0.5	91.83	69.30	–	45.41	**36.27**	88.59	104.38
	1	25.40	19.24	–	13.03	**12.39**	24.35	31.05
	2	4.66	5.22	–	**4.34**	4.93	4.66	5.42
	3	**1.90**	2.85	–	2.50	2.93	1.96	1.94
0.5	0	250.16	250.27	N/A	250.19	250.31	249.63	249.92
	0.5	106.98	86.84	–	68.80	**55.79**	105.58	115.10
	1	33.69	27.25	–	20.63	**18.54**	33.17	37.77
	2	6.45	7.03	–	**6.00**	6.64	6.55	7.08
	3	2.28	4.06	–	3.15	3.67	2.40	**2.23**
0.75	0	250.38	250.36	N/A	251.65	250.93	250.02	243.62
	0.5	131.04	114.61	–	108.88	**94.67**	130.11	130.71
	1	49.27	43.07	–	38.27	**33.71**	48.73	49.97
	2	10.13	10.37	–	**9.88**	10.46	10.24	10.27
	3	2.84	4.82	–	4.35	5.22	3.03	**2.54**
0.9	0	250.11	249.48	N/A	250.53	250.10	249.90	249.38
	0.5	158.02	146.87	–	151.04	**143.70**	157.59	158.07
	1	71.15	65.65	–	66.15	**62.03**	70.76	71.26
	2	**14.82**	15.02	–	16.34	17.32	15.14	14.92
	3	2.66	4.92	–	5.70	7.40	2.96	**2.11**

N/A : The in-control ARLs can not reach 250.

Bibliography

[1] Alwan, L. C. and Roberts, H. V. (1988). Time-series modeling for statistical process control. *Journal of Business and Economic Statistics*, **6**, 87-95.

[2] Bagshaw, M. and Johnson, R. A. (1975). The effect of serial correlation on the performance of CUSUM tests II. *Technometrics*, **17**, 73-80.

[3] Bohm, W. and Hackl, P. (1996). The effect of serial correlation on the in-control average run length of cumulative score charts. *Journal of Statistical Planning and Inference*, **54**, 15-30.

[4] Brook, D. and Evans, D. A. (1972). An approach to the probability distribution of cusum run length. *Biometrika*, **59**, 539-549.

[5] Fu, J. C. and Koutras, M. V. (1994). Distribution theory of runs: A Markov chain approach. *Journal of the American Statistical Association*, **89**, 1050-1058.

[6] Harris. T. J. and Ross. W. H. (1991). Statistical process control procedures for correlated observations. *The Canadian Journal of Chemical Engineering*, **69**, 48-57.

[7] Johnson, R. A. and Bagshaw, M. (1974). The effect of serial correlation on the performance of CUSUM tests. *Technometrics*, **16**, 103-112.

[8] Lu, C. W. and Reynolds, M. R., JR. (1999). EWMA control charts for monitoring the mean of autocorrelated processes. *Journal of Quality Technology*, **31**, 166-188.

[9] Lucas, J. M. and Saccucci, M. S. (1990). Exponentially Weighted Moving Average Control Schemes: Properties and Enhancement. *Technometrics*, **32**, 1-12.

[10] Montgomery, D. C. (2005). *Introduction to Statistical Quality Control*. Fifth edition, John Wiley & Sons, New York.

[11] Montgomery, D. C. and Mastrangelo, C. M. (1991). Some statistical process control methods for autocorrelated data. *Journal of Quality Technology*, **23**, 179-193.

[12] Runger, G. C. , Willemain, T. R. , and Prabhu, S. (1995). Average run lengths for CUSUM control charts applied to residuals. *Communications in Statistics, Part A – Theory and Methods*, **24**, 273-282.

[13] Schmid, W. (1997). CUSUM control schemes for Gaussian processes. *Statistical Papers*, **38**, 191-217.

[14] Tseng, S. and Adams, B. M. (1994). Monitoring autocorrelated processes with an exponentially weighted moving average forecast. *Journal of Statistical Computation and Simulation*, **50**, 187-195.

[15] VanBrackle, L. N. and Reynolds, M. R., JR. (1997). EWMA and CUSUM control charts in the presence of correlation. *Communications in Statistics – Simulation and Computation*, **26**, 979-1008.

[16] Vasilopoulos, A. V. and Stamboulis A. P. (1978). Modification of Control Chart Limits in the Presence of Data Correlation. *Journal of Quality Technology*, **10**, 20-30.

[17] Wardell, D. G., Moskowitz, H. and Plante, R. D. (1994). Run-length distributions of special-cause control charts for correlated processes. *Technometrics*, **36**, 3-17.

[18] Western Electric (1956). *Statistical Quality Control Handbook*. Western Electric Corporation, Indianapolis, IN.

[19] Woodall, W. H., and Faltin, F. (1993). Autocorrelated Data and SPC. *ASQC Statistics Division Newsletter*, **13**, 18-21. Birkhäuser, Boston.

[20] Yashchin, E. (1985a). On a unified approach to the analysis of two-sided cumulative sum control schemes with headstarts. *Advances in Applied Probability*, **17**, 562-593.

[21] Yashchin, E. (1985b). On the analysis and design of CUSUM-Shewhart control schemes. *IBM Journal of Research and Development*, **29**, 377-391.

[22] Yashchin, E. (1993). Performance of CUSUM control schemes for serially correlated observations. *Technometrics*, **35**, 37-52.

[23] Zhang, N. F. (1998). A statistical control chart for stationary process data . *Technometrics*, **40**, 24-38.